UC San Diego
UC San Diego Electronic Theses and Dissertations

Title

Profiling the effect of the proteasome inhibitor, carfilzomib, on gene expression in Schistosoma mansoni

Permalink

https://escholarship.org/uc/item/4809d2wq

Author

Denprasertsuk, Supacha

Publication Date

2021

Supplemental Material

https://escholarship.org/uc/item/4809d2wq#supplemental

Peer reviewed|Thesis/dissertation

UNIVERSITY OF CALIFORNIA SAN DIEGO

Profiling the effect of the proteasome inhibitor, carfilzomib, on gene expression in *Schistosoma mansoni*

A thesis submitted in the satisfaction of the requirements for the degree Master of Science

in

Biology

by

Supacha Denprasertsuk

Committee in Charge:

Professor Conor R. Caffrey, Chair

Professor Matthew Daugherty, Co-Chair

Professor Omar Akbari

2021

The thesis of Supacha Denprasertsuk is approved, and it is acceptable in quality and form for publication on microfilm and electronically.

University of California San Diego

2021

TABLE OF CONTENTS

LIST OF ABBREVIATIONS

WHO...World Health Organization

PZQ...Praziquantel

CFZ...Carfilzomib

BTZ...Bortezomib

OXO...Omaveloxolone

DMSO...Dimethyl Sulfoxide

qPCR...Quantitative Polymerase Chain Reaction

RNA-Seq...Ribonucleic Acid Sequencing

GEP..Gene Expression Profiling

LIST OF FIGURES

LIST OF TABLES

LIST OF SUPPLEMENTAL TABLES

ACKNOWLEDGEMENTS

ABSTRACT OF THE THESIS

Profiling the effect of the proteasome inhibitor, carfilzomib, on gene expression in *Schistosoma mansoni*

by

Supacha Denprasertsuk

Master of Science in Biology

University of California San Diego, 2021

Professor Conor R. Caffrey, Chair
Professor Matthew Daugherty, Co-Chair

Schistosomiasis is a neglected topical disease caused by trematode blood flukes of the genus *Schistosoma*. The disease affects impoverished communities with approximately 200 million people infected worldwide. Treatment of this disease relies on just one drug, praziquantel (PZQ). The high rates of reinfection, and concerns regarding the emergence of PZQ-resistant strains emphasize the need to identify new drugs and drug targets for schistosomiasis. The research presented here is part of a larger investigation by my research group, led by Dr. Caffrey, to

characterize the proteasome as a potential drug target for treatment of schistosomiasis. Using RNA-Seq, my thesis shows that several genes and gene families are up and downregulated in *Schistosoma mansoni* after exposure to 1 µM carfilzomib (CFZ) for 24 h, conditions which cause parasite immobility. Changes in gene expression by CFZ were compared with those generated by another proteasome inhibitor, bortezomib, and the non-proteasome inhibitor, omaveloxolone, which is an experimental drug for Friedreichs's ataxia. A number of genes and gene families, *e.g*., heat shock proteins, were upregulated by all three drugs tested, whereas other genes, specifically, the proteasome subunits and MEG-3 (micro-exon gene 3) proteins, were upregulated only after exposure to the proteasome inhibitors. Among the most downregulated genes common to all three drugs were those associated with the tegument (worm surface) and lipid metabolism. Changes in the -fold expression of exemplar genes by RNA-seq were validated by qPCR and, for the top 20 upregulated genes, I employed bioinformatics to understand their expression in different developmental stages of the parasite. The global data generated by my thesis provide a foundation to identify gene products which could be useful pharmacological targets, either independently or when combined with inhibition of the proteasome.

Introduction

1.1 Schistosomiasis: distribution and life-cycle

Schistosomiasis is a chronic and morbid parasitic disease caused by a trematode of the genus *Schistosoma* [1]. Approximately 200 million people are infected worldwide, and 700 million people are at risk of infection [2]. Highest infection rates are among children and adolescents. The disease impairs school performance which, in turn, can undermine social and economic development [3]. The three medically important species are *Schistosoma mansoni, Schistosoma haematobium* and *Schistosoma japonicum*. *S. haematobium* and *S. mansoni* occur in Africa and the Middle East, *S. mansoni* is present in South America, mainly in Brazil, and *S. japonicum* is found in Asia, especially parts of the Philippines and China [4].

Schistosomes are dioecious, meaning the parasite has separate male and female forms, which is unusual for flatworms [1]. Each mated female worm lays hundreds of eggs per day, of which approximately half are released in the feces (*S. mansoni/ S. japonicum*) or urine (*S. haematobium*); the other half is retained in host tissues [5]. In freshwater, the eggs hatch and release free-swimming miracidia (singular: miracidium) [6]. The miracidium searches for and penetrates the snail intermediate host and will asexually divide as mother and then daughter sporocysts. After four to six weeks, free-swimming cercariae are released into the water. Using its tail for propulsion, each cercaria searches for and penetrates the skin of the human definitive host, loses its tail and transform into young worms called schistosomula (singular: schistosomulum) [1; 4]. The schistosomulum migrates through the skin layers, enters the venous system and transits the lungs to reach the hepatic portal and mesenteric venous system. There, over the course of four to six weeks, the parasites mature and eventually mate [1; 4] (**Fig. 1**).
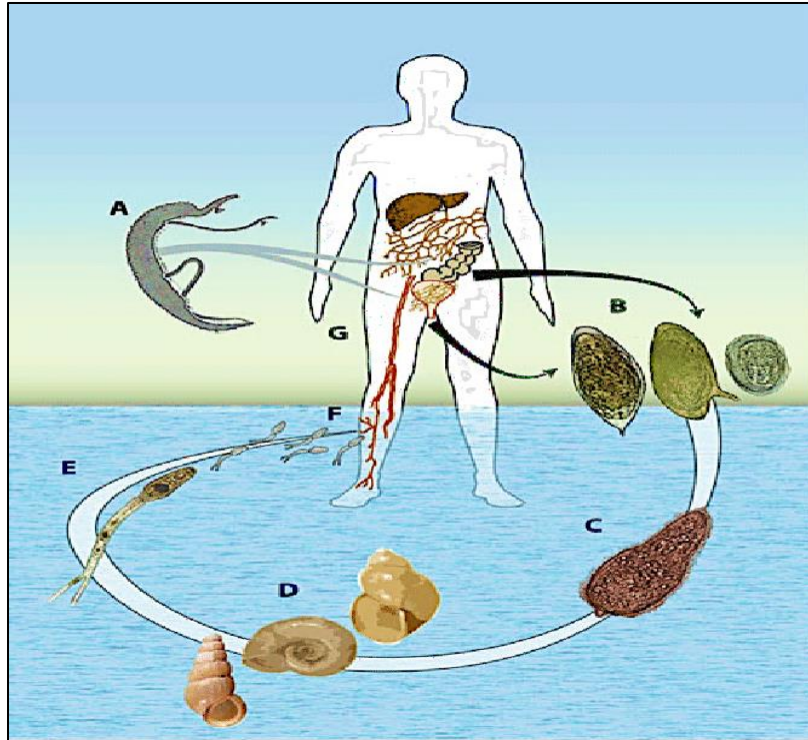
Figure 1. The developmental cycle of *S. mansoni, S. haematobium* and *S. japonicum*. The stages are indicated: (a) paired adult worms, (b) eggs (left to right: *S. haematobium, S. mansoni* and *S. japonicum*), (c) miracidium, (d) host snails (left to right, *Oncomelania*, *Biomphalaria* and *Bulinus*) and (e) cercariae: (f) and (g) indicate penetration and migration of the parasite through the skin and blood system, respectively, of the host. Taken from [7].

1.2 *Immunopathology, clinical symptoms and co-morbidities*

Schistosomiasis is associated with complex immune response mechanisms [1]. In the early stages of infection (the first 4-6 weeks), migrating schistosomula and immature adult worms provoke a T helper 1 (Th1) response by increasing the levels of pro-inflammatory cytokines such as TNF-α, IL-1, IL-6 and IFN-γ [8; 9]. As infection progresses, particularly with the onset of egg laying, a Th2-type response predominates with elevated levels of IL-4, IL-5, IL-10 and IL-13 cytokines [5; 8; 10].

Most of the immunopathology associated with infection is as a result of the host's immune responses to parasite eggs [11]. *S. mansoni* eggs secrete a variety of proteins such as IPSE (IL-4-

inducing principle of *S. mansoni* eggs), Omega-1 and proteolytic enzymes that drives a Th2 granulomatous inflammatory response which subsequently leads to fibrosis [12]. These events occur in both humans and mouse models of infection [13; 14]. IPSE is a glycoprotein [15] that has been identified as an activator of basophils and triggers the release of IL-4 and IL-13 [16-18]. Additionally, a recent study [19] shows a direct interaction between IPSE and B cells. Omega-1 is also a glycoprotein [20] and has been identified as a potent inducer of the Th2 response *in vitro* and *in vivo* [21; 22]. For example, Everts *et al.* [22] showed that Omega-1 initiates Th2 responses by lowering the production of IL-12 in dendritic cells.

Chronic infection with *S. mansoni* and *S. japonicum* cause hepatosplenic and hepato-intestinal disease [23; 24] whereby eggs trapped in the periportal spaces of the liver cause a variety of sequelae such as hepatic carcinoma, periportal fibrosis and liver fibrosis [4; 25]. Chronic infection associated with the deposition of *S. haematobium* eggs in the wall of the bladder and ureters causes ulceration and granulomatous inflammation of the urogenital tract [26; 27]. One major manifestation of *S. haematobium* infection is female genital schistosomiasis which is a concern for the World Health Organization (WHO) due to the increased risk of HIV infection [28]. A study performed in a rural Zimbabwean community found that women with genital schistosomiasis had a three-fold-increased risk of having HIV [29]. Infections with *S. haematobium* are also positively corelated with increased incidences of bladder cancer [30] and the International Agency for Research on Cancer has classified *S. haematobium* infection as carcinogenic [31]. A case-control study conducted in Alexandria, Egypt, found a 1.72-old increased risk of bladder cancer with *S. haematobium* infection [32].

1.3 *Current treatment*

Praziquantel (PZQ; 2 - (cyclohexylcarbonyl) -1,2,3,6,7,11b - hexahydro - 4H - pyrazino (2,1-alpha) isoquinolin-4-one) is the only drug recommended by the WHO for treatment and control of schistosomiasis (**Fig. 2**) [17]. First synthesized in the 1970s by Merck (Darmstadt, Germany), this failed analgesic was transferred to Bayer A. G. (Leverkusen, Germany) where its anti-trematodal activity was discovered and characterized [33]. PZQ is active against all schistosome species, and is safe and reasonably effective, having a cure rate of 60-90% and egg reduction rates of >90% when administered at the recommended single, 40 mg/kg oral dose [17; 18; 34]. The mechanism(s) of action of PZQ remains unclear, however, recent evidence suggests that the drug engages transient receptor potential (TRP) channels on the surface (tegument) of the parasite [35]. Exposure of the schistosome to sub-micromolar concentrations of PZQ causes a rapid uptake of calcium and damage to the tegument [36; 37]. This tegumental damage is thought to make the parasite susceptible to killing via the host's immune system [38].
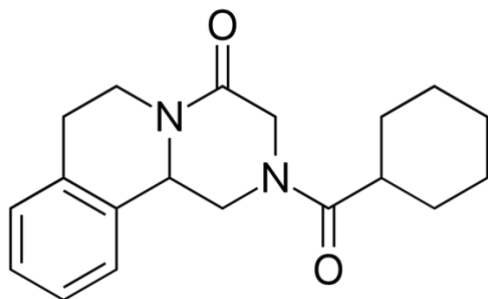
Figure 2. Chemical structure of praziquantel (PZQ). PZQ is also known as Biltricide® (Bayer HealthCare Pharmaceuticals Inc).

The reliance on just one drug to treat hundreds of millions of people afflicted with schistosomiasis calls into question the long-term sustainability of disease treatment and management, not least with the potential of drug-induced resistance [18]. There have been reports of possible resistance to PZQ. For example, in an outbreak of schistosomiasis mansoni in Senegal

in the late 1980s following construction of a dam, the cure rate for the standard 40 mg/kg dose 12 weeks after treatment was just 18%, *i.e.*, much less than the anticipated 60-90% [39; 40]. Also, resistance can be generated in laboratory mice [41]. Finally, PZQ is inactive against juvenile schistosomes which survive treatment and go on to reestablish infection once the drug has been removed from the body [42; 43]. Overall, therefore, there is an urgent need to identify novel drugs and drug targets to treat schistosomiasis.

1.4 The proteasome as an anti-parasitic drug target

The proteasome (**Fig. 3**) is a large multi-subunit protein complex located in the cytoplasm and nucleus of cells, and regulates protein turnover and degradation of misfolded proteins [44]. In eukaryotes, the 26S proteasome consists of a 20S barrel-shaped proteolytic core flanked by two 19S regulatory subunits (caps) [45]. The 20S core comprises two stacked rings of seven β subunits sandwiched between two rings of seven α subunits [45]. Three of the β subunits, β1, β2, and β5 have N-terminal threonine residues which are crucial for catalysis [46]. The β1 subunit is associated with caspase-like/ peptidylglutamyl-peptide hydrolyzing (PGPH) activities; β2 has a trypsin-like activity and β5 has a chymotrypsin-like activity [46]. The S1 pocket is a large hydrophobic binding site and is the major determinant of the specificities of the catalytic β subunits [47]. The PGPH specificity of β1 is attributed to the basicity of its S1 pocket which has Arg45 at its base; the trypsin-like activity of β2 is due to its S1 pocket having Glu53 at its base, and the chymotrypsin-like activity of β5 is due to its S1 pocket having Met45 at its base [47].
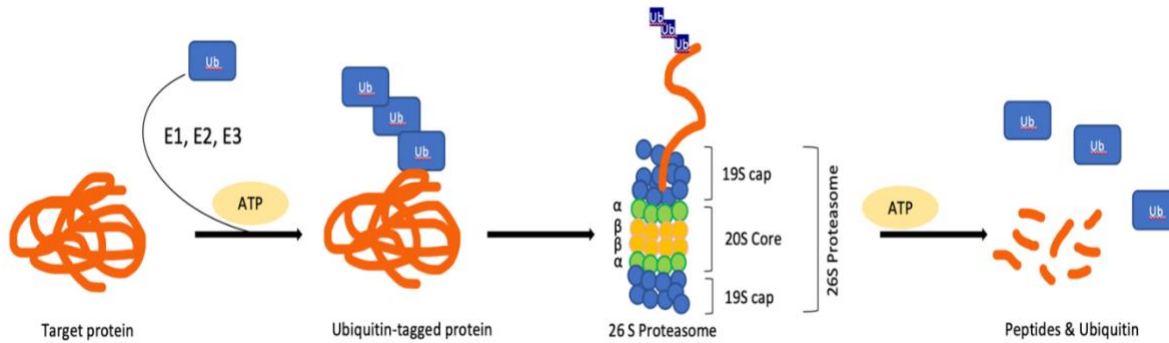
Figure 3. The ubiquitin-proteasome pathway. The target protein is ligated to a chain of ubiquitin (Ub) molecules via the E1, E2 and E3 ligases (ATP-dependent). On reaching the 19S cap, the target protein is unfolded and guided into the 20S core where it is degraded (ATP-dependent) to peptides that are recycled by the cell. The ubiquitin is recycled by the cell.

In eukaryotes, the ubiquitin (Ub)-proteasome pathway plays a major role in the recycling of cellular proteins [48] (**Fig. 3**). Initially, Ub-activating enzyme (E1) activates Ub at its C-terminus using energy provided by ATP. Ub-conjugating enzyme (E2) then transfers the activated Ub to the target protein to which it is conjugated via the Ub-ligating enzyme (E3). The target protein tagged with Ub chain then moves to the 26S proteasome where it is broken down into oligopeptides using energy from ATP. The Ub and peptides are recycled by the cell [48; 49].

Since the turn of the century, research has shown that the proteasome is a valuable drug target in the treatment of certain cancers, including multiple myeloma, and orally bioavailable proteasome inhibitors are currently used in myeloma treatment [50; 51]. One of these proteasome inhibitors, bortezomib (BTZ; **Fig. 4A**), is a reversible, dipeptide boronic acid inhibitor that binds to the nucleophilic threonine residue in the active site of the β5 subunit [52; 53]. This inhibition results in the activation of the unfolded protein response which involves the disruption of numerous cellular pathways, including those engaged in cell-signaling and -division, and apoptosis, which eventually leads to cell-death [54]. BTZ has also been studied in a number of cancer clinical trials including for non-Hodgkin's lymphoma and ovarian cancer [55; 56].
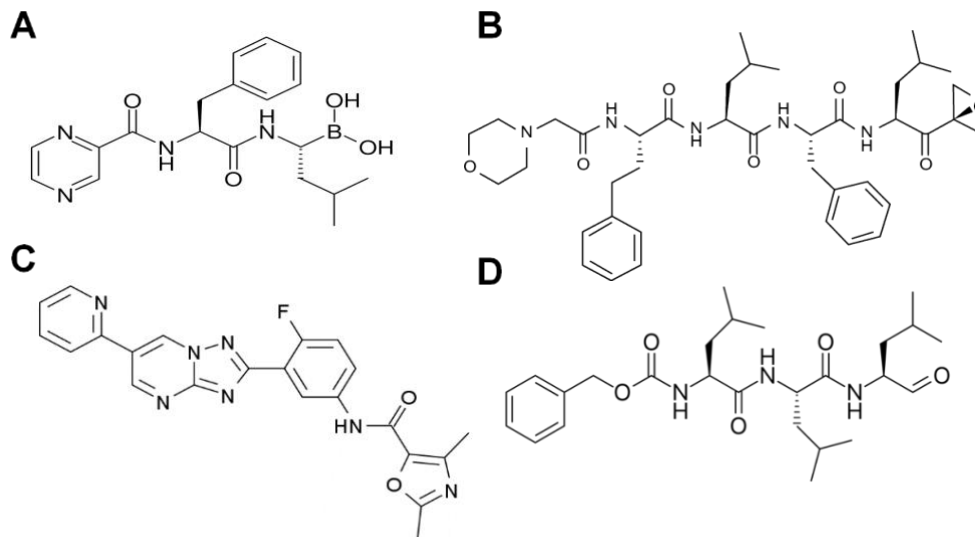
Figure 4. Chemical structures of BTZ, CFZ, GNF6702 and MG132. BTZ (**A**) is marketed as Velcade® by Takeda Pharmaceuticals Inc. and is used to treat multiple myeloma [57]. CFZ (**B**) is marketed as Kyprolis® by Onyx Pharmaceuticals Inc. and is used in multiple myeloma patients who are treatment-refractory to BTZ and immunomodulatory agents [58]. GNF6702 (**C**) is an allosteric inhibitor of the kinetoplastid proteasome under development for treatment of kinetoplastid infections [59]. MG132 (**D**) is a reversible peptide-aldehyde proteasome inhibitor that induces apoptosis in tumor cells [60].

Carfilzomib (CFZ; **Fig. 4B**) is an irreversible, epoxyketone tetrapeptide inhibitor that primarily inhibits the β5 subunit [61]. CFZ is active against BTZ-resistant cell lines [62]. CFZ is 100-fold and 1000-fold more selective for β5 over β1 and β2, respectively, whereas BTZ inhibits the β5 and β1 subunits with equal potency [63]. This selectivity of CFZ combined with its more limited off-target effects [64] means that CFZ is less toxic than BTZ [65; 66].

Using small molecule inhibitors, the proteasome has been established as a valuable drug target *vs.* parasitic infections caused by *Plasmodium* malaria and *Leishmania* [59; 67; 68]. For instance, GNF6702 (**Fig. 4C**) reduced the liver burden of *Leishmania donovani* in mice by 90% and it eradicated parasites in mice infected with *Trypanosoma brucei* or *Trypanosoma cruzi* [59].

For *S. mansoni*, exposure of cercariae to 50 μM of the proteasome inhibitor, MG132 (**Fig. 4D**), decreased by 96% the parasite's ability to establish infection [69]. Subsequently, research by

the teams of my supervisor, Dr. Caffrey and his SSPPS faculty colleague, Dr. Anthony O'Donoghue, has shown that 1 µM of BTZ and CFZ decreased the motility of *S. mansoni* adults by 45% and 47% after 6 h, and by 87% and 89% after 24 h, respectively. These phenotypic effects correlated with a >90% decrease in the catalytic activity of the parasite's proteasome (termed Sm20S) [63]. By 72 h, the parasites were dying and an increase in apoptosis-inducing caspase activity, a hallmark of the interruption of proteasome activity [70], was recorded (>4.5-fold over non-treated control worms [63]). These data suggest that Sm20S has potential as a drug target and further investigation is warranted.

1.5 Goals of this thesis.

Proteasome inhibitors kill the schistosome. Thus, my thesis is part of a larger project by my lab that investigates the effect of CFZ, BTZ and non-proteasome inhibitor drugs on the transcriptomic response of *S. mansoni* with the aim of identifying new molecular targets for drug development.

For my thesis I will:

1. Identify and characterize genes among the top 300 genes that are upregulated or downregulated after *in vitro* exposure of adult male *S. mansoni* to 1 µM CFZ, BTZ or 0.5 µM of the non-proteasome inhibitor drug, omaveloxolone (OXO). RNA-Seq was used to generate the respective data sets (El-Sakkary et al., 2021, *manuscript in preparation*). Data for CFZ and OXO are analyzed here for the first time whereas data for BTZ had previously been analyzed by our lab and are incorporated here for comparison [71].

2. Among the top 300 genes that are upregulated or downregulated, manually characterize those genes that had originally been annotated as 'uncharacterized' or 'unknown' in *S.*

mansoni genome. This is important to provide as comprehensive a data set as possible for interrogation and comparison

3. For a small number of genes, use qPCR to validate the CFZ-induced upregulation of transcription as measured by RNA-Seq

4. Compare selected genes that are up and downregulated after exposure to proteasome inhibitors and/or OXO.

5. Analyze the distribution of selected gene transcripts that are upregulated after exposure to CTZ across different developmental stages of the parasite.

3. Materials and Methods

3.1 Maintenance of the *S. mansoni* life cycle

The National Medical Research Institute (NMRI) isolate of *S. mansoni* was cycled between the intermediate snail host, *Biomphalaria glabrata,* and a definitive mammalian host, specifically, the Golden Syrian hamster, *Mesocricetus auratus* (Charles River Labs, Wilmington, MA) [72]. Animals were maintained in accordance with protocols approved by UC San Diego's Institutional Animal Care and Use Committee (IACUC). Infections with *S. mansoni* were initiated by subcutaneous injections of 4-6-week-old female hamsters with 600-800 cercariae. Six weeks post-infection, hamsters were euthanized with a single intra-peritoneal (i.p.) injection of 100 mg/kg Fatal-Plus (pentobarbital solution; Vortech Inc.). Adult worms were harvested by reverse perfusion of the hepatic portal system in RPMI 1640 medium containing 700 U heparin (Thermo Fisher Scientific Inc., MA, USA) [72].

3.2 Exposure of adult *S. mansoni* to proteasome inhibitors *in vitro*

CFZ (Ubiquitin-Proteasome Biotechnologies, UBPBio LLC., CO, USA) and OXO (MedChemExpress LLC., NJ, USA, HY-12212) were purchased commercially. OXO is not a proteasome inhibitor and was employed to compare its effects on the *S. mansoni* transcriptome with those of CFZ and BTZ (**Fig. S1**). OXO is an antioxidant oleanane triterpenoid currently undergoing clinical trials for treatment of Friedreich's Ataxia [73]. All drugs were stored as 10 mM solutions in pure DMSO at – 80ºC until use.

After perfusion, worms were washed five times in Basch medium 169 containing 1x penicillin-streptomycin solution and 10 µg/mL amphotericin B (Thermo Fisher Scientific Inc., MA, USA) [74] under sterile conditions. After three further washes without amphotericin B, parasites were manually dispensed into 24-well culture plates (Corning™ 3526; NY, USA) at approximately five males/well in 0.5 ml medium. The volume was made up to 1 ml with the same medium containing 4% fetal bovine serum (FBS; Thermo Fisher Scientific Inc., MA, USA) and the parasites were incubated at 37 ºC and 5% CO_2 for up to 18 h to acclimate prior to addition of drug.

CFZ or OXO was added at a final concentration of 1 or 0.5 µM, respectively, to the parasite cultures and the final volume made up to 2 ml with Basch medium containing 4% FBS and 1x penicillin-streptomycin. The final concentration of DMSO was 0.5%. Controls were established under the same conditions but in the absence of drugs. Parasites were incubated at 37 ºC and 5% CO_2 for 24 h, washed five times in cold PBS and flash frozen in ethanol-dry ice for storage at – 80 C. After 24 h, worms exposed to CFZ are immobilized and are not attached to the well bottom via the ventral sucker; by 72 h the worms are dying or dead. For OXO, worms display uncoordinated movements and show signs of degeneracy (including a damaged outer surface) after 24 h; by 48

h, the worms are dead. CFZ experiments were derived from three separate perfusions each performed in triplicate whereby two wells, each containing 5 males, were combined for each RNA-Seq sample. OXO experiments were derived from one perfusion and experiments were set up as described for CFZ.

3.3 RNA Extraction

Ten worms were combined to prepare one RNA sample with a minimum of three RNA samples per perfusion. For RNA extraction, worms were placed into 1.5 mL tubes (Thermo Fisher Scientific, MA, USA), washed four times in PBS, resuspended in 50 µL TRIzol (Thermo Fisher Scientific, Inc., MA, USA), snap frozen over dry ice and stored at –80°C. Worms in 800 µL TRIzol were homogenized with a pestle and the homogenate was transferred to a 2 mL tube containing zirconia-silica beads (#S6012-50, Zymo Research, CA, USA). The homogenate was vortexed in a Fisher Scientific Analog Vortex Mixer (Cat #02215365, Model # 945404, Waltham, MA, USA) at the maximum setting (50160 Hz = 1 phase) for 6 min, placed on ice for 2 min, and the procedure repeated. Pure ethanol was added, and the homogenate added to the kit-provided column (Direct-zol RNA Miniprep, #R2051, Zymo Research, CA, USA). The sample was then washed, and the RNA isolated according to the manufacturer's kit instructions.

3.4 RNA-Sequencing (RNA-seq) Sample Quality Control

Using a Nanodrop (ND2000, Thermo Fisher Scientific, Inc., MA, USA), the absorbance of samples was measured at 260 nm to calculate the RNA concentration (minimum 50 ng/µl acceptable) and the 260 nm : 280 nm (RNA : protein) ratio was used to determine purity, whereby a ratio ≥1.8 was considered acceptable. Additional quality assessment was performed at the UC

11

San Diego Institute for Genomic Medicine (IGM) services center (La Jolla, CA, USA) using an Agilent 2100 Bioanalyzer (Agilent Technologies, CA, USA). The bioanalyzer separates fluorescently-bound RNA based on size using microfluidics in microchannels to generate an electropherogram output that indicates fluorescent units (FU). Ribosomal (r)RNA is used as an indicator of RNA quality. To evaluate the RNA quality, we compared the electropherogram 18S peak intensity (>4000 FU) relative to the fluorescence of other RNA in the sample (<1000 FU). This method was used as schistosomes lack 28S rRNA which is typically compared to 18S rRNA to assess RNA quality via the generation of a RNA Integrity Number (RIN) [75].

3.5 RNA-Seq

Five cDNA libraries per RNA-Seq run were prepared for both CFZ and BTZ, and three cDNA libraries were prepared for OXO. cDNA library constructs and adaptor-ligated gene fragments were synthesized at the IGM using 100 ng of RNA per library. Each library was synthesized using the TruSeq Stranded Total RNA Ribo-Zero H/M/R Gold kit (Illumina Inc., CA, USA). Libraries were sequenced in an Illumina HiSeq 4000 sequencer using single-end reads (SR75).

Data from each sequencing run were visualized on a Bland–Altman plot (MA) plot generated using the ROSALIND^TM software (OnRamp Biotechnologies Inc, San Diego, CA). The MA plot visually represents genomic data across different sequencing runs. The plot displays M (log ratio) and A (mean average) scales to determine differences between measurements taken across sequencing runs. The fold change in expression across the sequencing runs for each of the drugs tested displayed the same patterns although with different absolute expression values, which

are attributable to slight environmental and handling differences. Ultimately, one sequencing run was selected for each of the drug-treated samples for gene expression profiling.

3.6 RNA-Seq analysis

RNA-Seq data were generated in the FASTq format with each file being approximately 500 MB in size. Files were analyzed using ROSALIND™ [41] which uses a proprietary HyperScale architecture to map reads. Each library was normalized by determining the Relative Log Expression (RLE) using Differential Gene Expression (DESeq2) analysis based on the negative binomial distribution [76]. DESeq2, available as a package in R (RStudio, Boston, MA), was used to calculate relative gene expression (fold changes; ≥1.5 fold considered significant) compared to DMSO controls and the associated p-Adjusted (P-Adj) values (≤0.05 cutoff). DESeq2 automatically identifies outlier genes using Cooks' distance and removes these from the analysis [77]. Upon determining the fold-expression changes and P-Adj values, Partitioning Around Medoids (PAM) was used to partition RNA-Seq data into heat-maps. The PAM algorithm organizes the RNA-Seq data by clustering genes into groups with similar expression profiles [78].

Enrichment analysis of pathways, gene ontology and domain structure were performed with ROSALIND using the Hypergeometric Optimization of Motif EnRichment (HOMER) tool [79]. HOMER is available online (http://homer.ucsd.edu/homer/) and allows RNA-Seq data to be mapped to the *S. mansoni* genome (Version 7, Wellcome Trust Sanger Institute, UK) and analyzed using thousands of built-in commands.

3.7 Homology analysis

Gene identification is made difficult for *S. mansoni* by the fact that approximately 44% of the genes in the genome are annotated as 'hypothetical' or 'uncharacterized.' Focusing on the top 300 genes that were either upregulated or downregulated relative to control (P-Adj $\geq$ 0.05), it was necessary to attempt manual annotation to enrich the dataset. The Basic Local Alignment Search Tool (BLAST) tool, a sequence similarity search program available through the National Center for Biotechnology Information's (NCBI) web interface (http://www.ncbi.nlm.nih.gov/BLAST) [80], was employed. Specifically, BLAST searches for regions of local similarity between nucleotide or amino acids and approximates alignments via the optimum maximal segment pair (MSP) score.

Each *S. mansoni* 'Smp' gene identifier characterized as 'hypothetical' or 'uncharacterized' was interrogated using the BLASTn (nucleotide-to-nucleotide sequence search) and BLASTp (protein-to-protein sequence search) programs. Search returns were filtered based on percent identity (40% minimum), query coverage (40% minimum) and lowest Expect (E)-value (a measure of the probability of observing the results by chance). BLASTn results were prioritized over those of BLASTp because nucleotides (nts), encoding three nts to an amino acid (AA), provide more information to compare and evaluate the evolutionary relationships between sequences of interest. When a BLAST search did not return sequence data that met our minimum criteria, the Smp gene identifier was searched via the Universal Protein Resource or UniProt (https://www.uniprot.org/), a comprehensive resource of protein sequence and annotation data [81]. The Smp gene identifier was specifically queried against the UniProt Knowledgebase (UniProtKB), one of the three UniProt databases. Because we were interested in annotating genes based on their functional information (*i.e.*, amino acid sequence, protein name, protein description, taxonomic data and

citation information), UniProtKB was used in preference to UniRef, which provides clustered sets of sequences from UniProtKB, and UniParc, which only contains protein sequences [81]. Gene sequences meeting the filter criteria were handled in Microsoft Excel as described in the supplemental data (page 35).

3.8 Functional annotation of up and downregulated genes

To functionally annotate the top 300 upregulated and downregulated genes, we utilized the Kyoto Encyclopedia of Genes and Genomes (KEGG) (www.genome.jp/kegg) [82]. KEGG comprises eighteen databases broadly organized into four categories: (i) systems information, (ii) genomic information, (iii) chemical information and (iv) health information. Each of the 300 upregulated and downregulated genes was inputted into all four of the KEGG database categories. The KEGG Orthology (KO) output was recorded and the genes were then grouped into the following KEGG pathway categories: metabolism, genetic information processing, environmental information processing, cellular processes, organismal systems and human diseases.

3.9 cDNA Synthesis prior to quantitative real-time PCR (qRT-PCR)

Worms were incubated with drug or DMSO, as described in Section 3.2. Total RNA was extracted using a kit (#R2051, Zymo Research®, CA, USA) and cDNA synthesized from 1 μg RNA using the SuperScript™ VILO cDNA Synthesis Kit (#11754050, Thermo Fisher Scientific Inc., MA, USA) according to the manufacturer's protocol. The cDNA concentration was determined via Nanodrop. The 260 nm : 230 nm and 260 nm : 280 nm wavelength ratios were measured, and respective values of 1.60-1.90 and 1.90-2.05 indicated minimal contamination by carbohydrate, or phenol and protein, respectively [83]. Samples were frozen at –80°C.

3.10 Design of primers for qPCR validation of selected upregulated gene transcripts

Primer efficiency ensures that cDNA amplification with a specific primer set under a set of qPCR conditions is as close to 100% as possible such that the data arising accurately reflect mRNA abundance [84]. As part of his recent Master's thesis, my colleague, Ali Syed, had previously designed forward and reverse primers for 12 genes (including two control gene transcripts unaffected by proteasome treatment) using the NCBI primer design tool [85] (**Table 1**). Primers had no more than 12 consecutive nucleotides that paired with other genes in the *S. mansoni* genome to minimize non-specific binding. Primers were also selected based on a GC content >55%. As determined previously by Ali Syed, primer efficiencies ranged between 92 and 114%. These primers were used to validate the upregulation of the target genes in response to incubation of adult *S. mansoni* with 1 µM CFZ for 24 h, as described in Section 3.2.

Table 1. Gene targets for qPCR validation and their final primer efficiencies

Gene ID[a]	Category	Gene Description	Fold Change	P-Adj Value	Primer Efficiency
Smp_049250	Stress Response	HSP20/α-crystallin family	29.40	7.02E-66	107%
Smp_106930	Stress Response	HSP 70 kDa homolog	18.48	5.63E-55	92%
Smp_123260	Apoptosis/Proteasome Pathway Genes	Ubiquitin 1	4.11	3.48E-15	114%
Smp_171150	Cell Regulation	Shk1 kinase-binding protein	2.54	2.68E-19	112%
Smp_102240	Cell Regulation	Upf3 regulator of nonsense transcripts-like protein	2.05	6.89E-20	107%
Smp_072340	Proteasome	26s proteasome regulatory subunit 6b	2.12	7.61E-09	105%
Smp_052870	Proteasome	26s proteasome non-ATPase regulatory	1.90	4.03E-15	112%
Smp_119310	Proteasome	26s protease regulatory subunit	1.73	3.51E-17	103%
Smp_067890	Proteasome	Proteasome subunit α-type	2.06	7.99E-18	107%
Smp_025800	Proteasome	Proteasome subunit b-type	1.57	5.83E-12	108.7%
Smp_165020	Control	Transmembrane 9 superfamily protein member	1.00	N/A	112%
Smp_044920	Control	Dynamin	1.00	N/A	114%

[a]Nine target and two control gene transcripts were used for amplification by qPCR. By RNA-Seq, the nine target transcripts were determined to be significantly upregulated with a fold change ≥ 1.5 and a P-Adj value ≤ 0.05. Data courtesy of Ali Syed.

3.11 q-PCR

RNA-Seq technology requires RNA to be fragmented to make double stranded cDNA, a process that could result in both positional and sequence-specific bias that can affect expression estimates [86]. Therefore, qRT-PCR was employed as a secondary method to validate the expression levels of candidate genes measured by RNA-Seq. cDNA was generated as described above. qPCR was performed in an Mx3005p thermocycler (Agilent Technologies, CA, USA). Samples were prepared in a 20 μl volume containing 10 μL of PowerUp SYBR™ Green Master Mix (Thermo Fisher Scientific Inc., MA, USA), 1.4 μL of each of the forward and reverse primers, 1uL of cDNA, and 6.2 μL of water. Two genes, Smp_165020 (transmembrane 9 superfamily protein) and Smp_044920 (dynamin), were selected as internal controls because they were unaffected by drug treatment.

17

Relative gene expression was calculated using the comparative ΔΔCT method [87]. Briefly, the threshold cycle (Ct) values obtained from different RNA samples are normalized using the control genes, Smp_165020 and Smp_044920, before comparison [87]. This method compares the number of PCR cycles needed to reach a threshold amount of amplification, calculated as relative fluorescence units (RFU), in our case 3,000 RFU. In comparison to control genes, upregulated genes would need a lower number of PCR cycles to reach the threshold.

4. Results

4.1 Gene expression profiling and functional annotations

Adult male *S. mansoni* was incubated for 24 h in the presence of 1 µM of the proteasome inhibitors, BTZ or CFZ, or the experimental antioxidant drug, OXO. Worms were then washed and processed for RNA-Seq. Data arising from the treatment with BTZ have been presented by Ali Syed as part of his recent Master's thesis [71] and are used here for comparative purposes.

Of the approximately 3,000 genes differentially expressed relative to DMSO controls, the top 300 up and downregulated genes were further examined. At the outset, 39% (118/300 genes) and 44% (131/300 genes) of the up and downregulated genes, respectively, had been annotated in the *S. mansoni* genome (Version 7, Wellcome Trust Sanger Institute, UK) [88] as 'hypothetical' or 'uncharacterized.' After employing manual BLAST homology analysis, the respective percentages remaining in these categories were reduced to 12% (36/300 genes) and 9% (26/300 genes).

Approximately half of the top 300 upregulated genes were identified by KEGG analysis as those involved in the category, Genetic Information Processing, with smaller proportions associated with the other major categories, including cellular processes, organismal systems and

environmental information processing (**Fig. 5A**). Within the genetic information processing category, many of the identified sequences regulate molecular functions such as transcription (38%), ubiquitin-mediated proteolysis (13%), heat shock (5%) and DNA repair (4%; **Fig. 5B**).
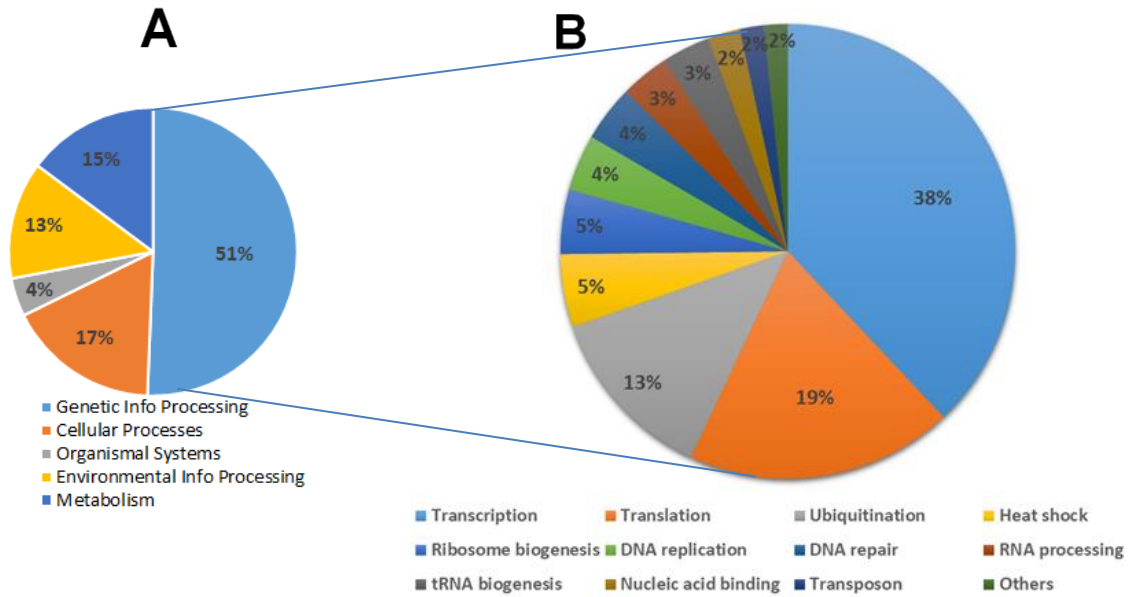
Figure 5. Pie chart representations of the top 300 genes upregulated after incubation with CFZ. Indicated are the proportions of genes associated with the (A) primary and (B) secondary KEGG categories, the latter of which are broken out from the Genetic Info Processing portion.

Conversely, for the top 300 genes that were differentially downregulated, there was a roughly even split among the different KEGG categories (**Fig. 6**).
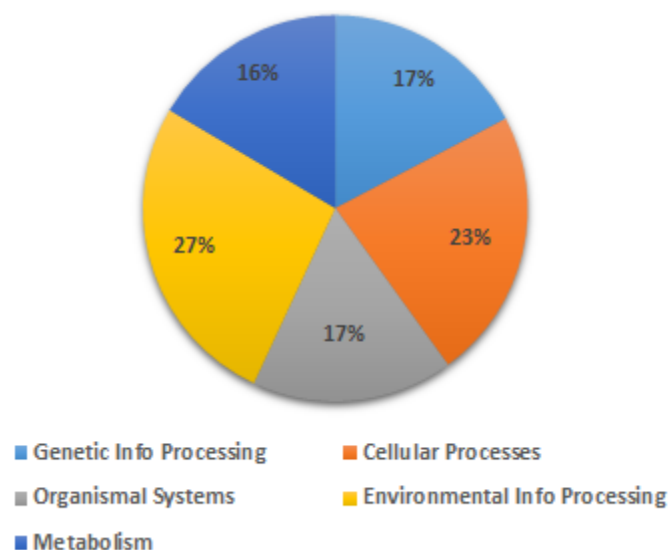
Figure 6. Pie chart representation of the top 300 genes most downregulated after treatment with CFZ. The proportion of genes associated with each primary KEGG category is shown.

Similarly, in the case of OXO-treated worms, approximately half of the top 300 upregulated genes were identified by KEGG analysis as those involved in genetic information processing with the remainder belonging to the other primary categories, namely, cellular processes, organismal systems and environmental information processing (**Fig. 7A**). Within the genetic information processing category, many of the identified sequences regulate molecular functions, such as transcription (28%), translation (12%), ubiquitination (11%) and DNA replication (11%) (**Fig. 7B**).

For the top 300 genes that were differentially downregulated, there was once again an even split in distribution among the different KEGG categories (**Fig. 8**).
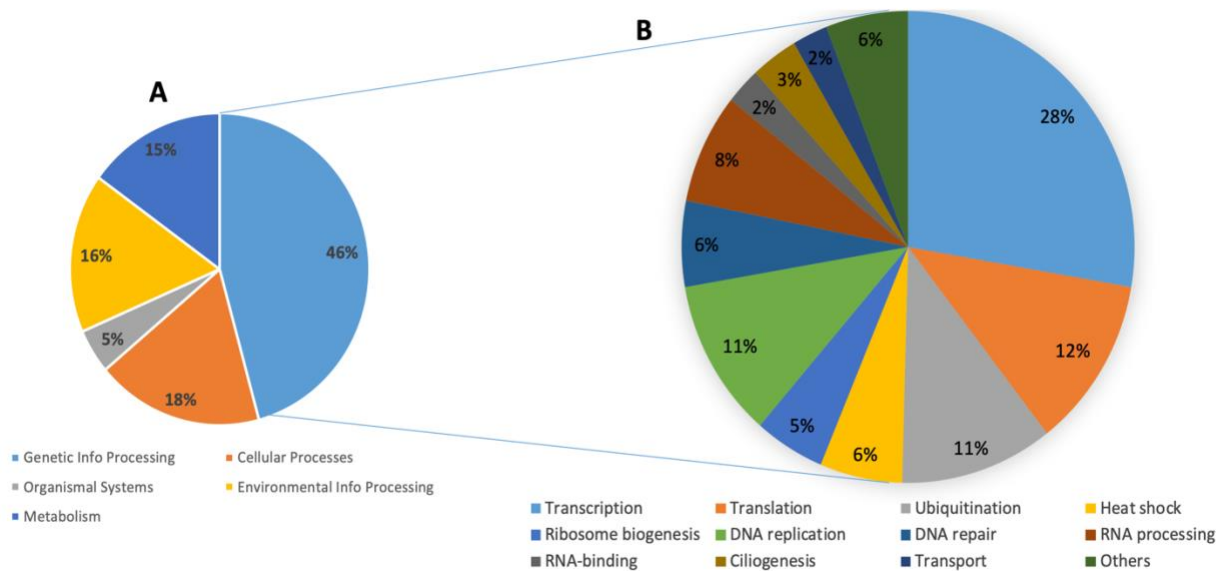
Figure 7. Pie chart representations of top 300 genes upregulated after incubation with OXO. Pie charts showing the proportions of genes associated with the (A) primary and (B) secondary KEGG categories, the latter of which are broken out from the genetic info processing portion.
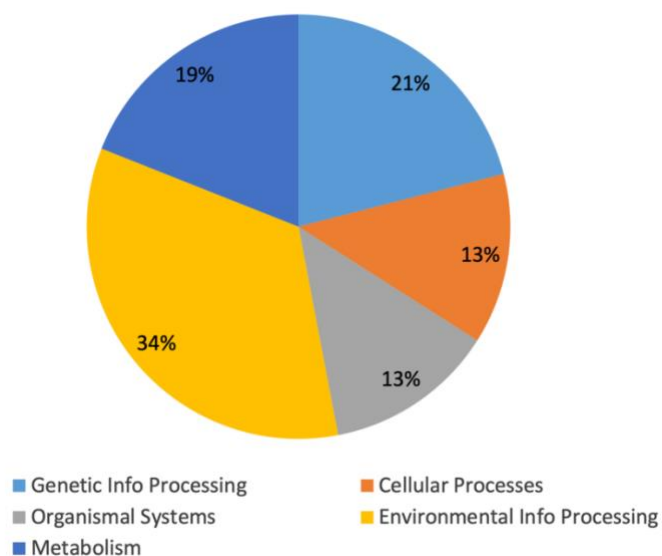
Figure 8. Pie chart representation of the top 300 genes downregulated after treatment with OXO. The proportion of genes associated with each KEGG pathway is shown.

For the top 300 differentially expressed genes following treatment with BTZ and CFZ, 166 genes were commonly upregulated (the intersectional area of the Venn diagrams in **Fig. 9A**)

whereas 134 were unique to either treatment. For the downregulated genes, 127 transcripts were

shared whereas 173 transcripts were unique to either treatment (**Fig. 9B**). Considering OXO, for

the upregulated genes, 56 transcripts were shared with BTZ and 72 shared with CFZ, with 224

OXO-specific gene transcripts (**Fig. 9B**). For the downregulated genes, 67 transcripts were shared

with BTZ and 80 were shared with CFZ, with 188 OXO-specific gene transcripts (**Fig. 9B**). For

both the upregulated and down regulated genes, the data suggest that both proteasome inhibitor

treatments have more genes in common than with the OXO treatment.
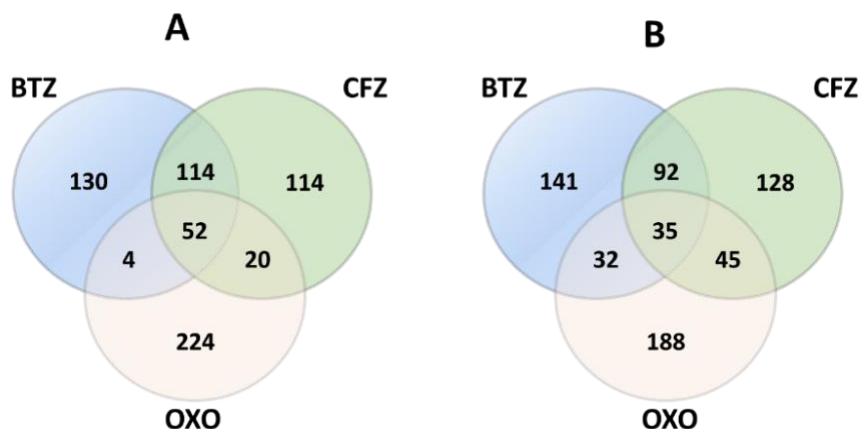
Figure 9. Venn diagram analysis of differentially expressed genes following exposure to BTZ, CFZ or OXO. (**A**) upregulated gene transcripts, (**B**) downregulated gene transcripts.

The 10 gene transcripts that were most upregulated or downregulated following treatment with the

three drugs, and their KEGG pathway associations, are listed in **Tables 2** and **3**, respectively.

Table 2. The 10 most upregulated genes after treatment with CFZ, BTZ or OXO

Smp ID	Description	Fold Change CFZ	Fold Change BTZ	Fold Change OXO	Molecular Function	KEGG Pathway
Smp_185680*	Major Egg Antigen	35.6	5.58	21.8	Immune	OS[b]
Smp_049250	HSP20/Alpha Crystallin Family	29.4	11.5	11.1	Heat shock	GIP
Smp_138060	MEG-3 (Grail) Family	23.1	4.5	n.p.[a]	Immune	OS
Smp_106930	HSP70 kDa	18.5	13.2	10.9	Heat shock	GIP
Smp_049300	Major Egg Antigen	15.6	5.9	13.2	Immune	OS
Smp_003600*	Natterin-4 Protein	11.1	4.4	6.0	Toxin	CP
Smp_048050	Alpha Crystallin A chain / HSP Beta-4	10.5	6.0	3.1	Heat shock	GIP
Smp_149750*	Vacuolar Sorting Associated Protein 11	9.7	7.6	41.0	Transport	CP
Smp_049230	HSP16	8.6	5.6	3.3	Heat shock	GIP
Smp_049240	HspB1; HSP27	7.8	4.2	19.4	Heat shock	GIP

*These genes were manually characterized via BLASTn analysis.

[a]n.p.: not present in the particular dataset.

[b]Key: Genetic Information Processing (GIP); cellular processes (CP); organismal systems (OS).

Table 3. The 10 most downregulated genes after treatment with BTZ, CFZ or OXO

Smp ID	Description	Fold Change CFZ	Fold Change BTZ	Fold Change OXO	Molecular Function	KEGG Pathway
Smp_017610	Amine Oxidase	-17.8	n.p.[a]	-7.8	Amino Acid Metabolism	M[b]
Smp_195090	Tegumental Antigen (SmTAL5 gene)	-14.7	-2.3	-2.1	Immune	OS
Smp_123550	Venom Allergen-like (VAL) 8 Protein	-14.3	n.p.	-9.0	Immune	OS
Smp_017620	Membrane Primary Amine Oxidase	-13.0	n.p.	-6.2	Amino Acid Metabolism	M
Smp_164550	Hypothetical Protein	-12.8	n.p.	-17.4	Unc	Unc
Smp_203440	Hypothetical Protein	-12.2	n.p.	-25.9	Unc	Unc
Smp_086530	Tegumental Protein	-11.4	n.p.	-3.4	Immune	OS
Smp_141500	*Schistosoma* spp. Protein UPF0506	-10.6	n.p.	-27.2	Unc	Unc
Smp_196730	Malignant Fibrous Histiocytoma-amplified Sequence 1	-9.7	-3.1	-2.5	Immune	OS
Smp_156930	Hypothetical Protein	-9.4	n.p.	-3.6	Unc	Unc

*These genes were manually characterized via BLASTn analysis.
[a]n.p.: not present in the particular dataset.
[b]Key: organismal systems (OS); metabolism (M); uncharacterized (Unc).

4.2 Primer efficiency and validation of RNA-Seq data

Twelve primer pairs (ten differentially expressed genes and two unmodulated control genes), previously designed by Ali Syed of our lab, were tested by qPCR on cDNA that had been derived from adult male *S. mansoni* exposed to 1 µM CFZ for 24 h. The data generated for the fold change in the upregulation of all ten genes of interest by qPCR agreed with those measured

by RNA-Seq (**Fig. 10**) and the agreement is statistically significant. Thus, the qPCR data suggest that the RNA-seq data are, as a whole, accurate.
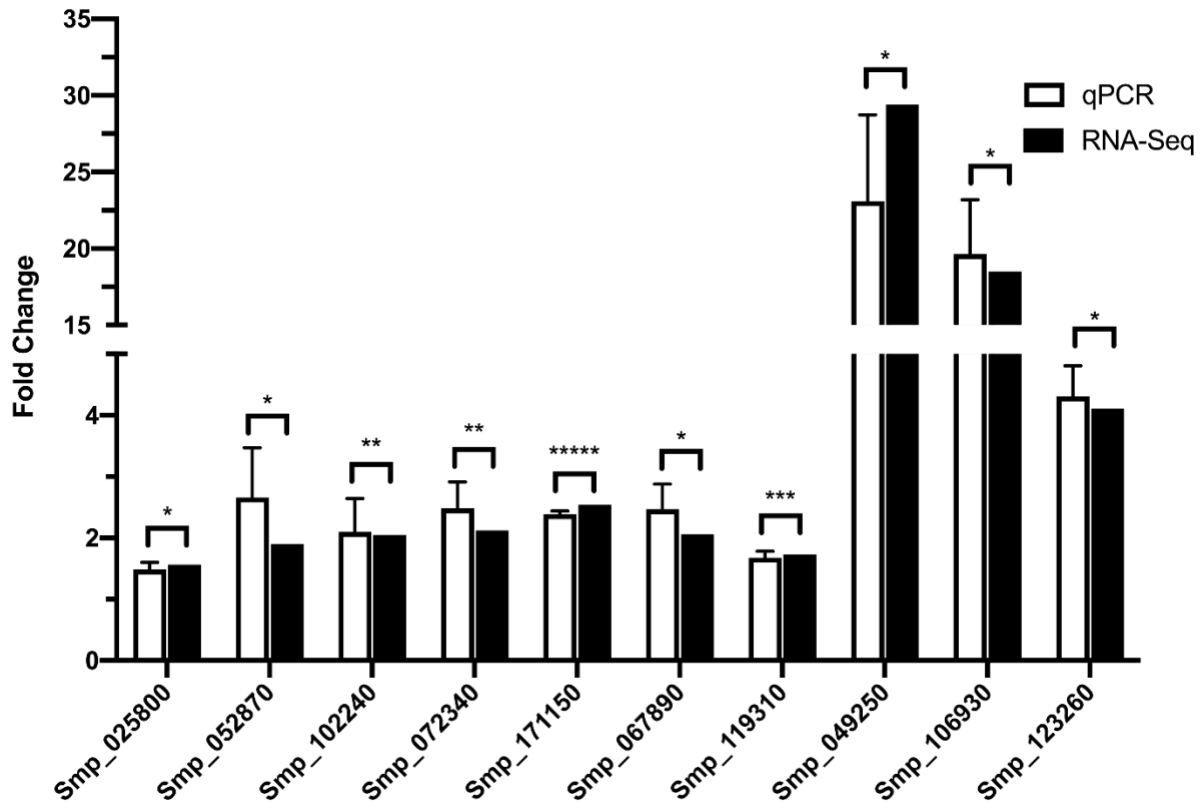
Figure 10. Comparison of fold changes in expression of selected genes by qPCR and RNA-Seq after incubation of *S. mansoni* adult males with 1 μM CFZ 24 h. Experiments were analyzed using the ΔΔCT methodology [87]. Smp_044920 and Smp_165020 were employed as control genes, *i.e.*, for which expression is not altered from control. The means and standard error of the means (SEMs) are shown for two biological replicates each performed in triplicate. Student's two-sided *t*-tests were performed to measure the statistical significance between the qPCR and the RNA-Seq data; *p=<0.05, **p=<0.005, ***p=<0.0005 and ***** p=<00000.5

4.3 Stage-specific expression of genes exposed to CFZ for 24 h

For the top 20 genes upregulated after exposure to CFZ for 24 h and the ten target genes validated by qPCR (**Fig. 10**), we used the NCBI BLASTn and BLASTp tools to query the *S. mansoni* expressed sequence tag (EST) data, and understand whether the genes of interest were expressed in other developmental stages of the parasite (**Table 4**). Genes encoding heat shock

proteins (HSPs) and proteasome subunits were widely distributed whereas other genes were less

so, although this might be due to the data being simply unavailable for the particular life-stage.

Table 4. Developmental stage expression of the top 20 upregulated genes and the ten qPCR genes after exposure to CFZ for 24 h

Name	Description	Fold Change	P-Adj	ME[a]	MG	ML	MS	MC	MA	MF
Smp_185680	Uncharacterized protein	35.55	1.56E-39							
Smp_049250*	HSP20/alpha crystallin family	29.40	7.02E-66							
Smp_138060	MEG-3 (Grail) family	23.09	1.10E-28							
Smp_106930*	HSP 70 kDa homolog	18.48	5.63E-55							
Smp_049300	Major egg antigen	15.79	8.98E-16							
Smp_003600	Uncharacterized protein	11.14	2.15E-22							
Smp_048050	Alpha crystallin A chain	10.48	5.06E-41							
Smp_149750	Uncharacterized protein	9.69	8.75E-19							
Smp_049230	HSP16	8.56	4.53E-52							
Smp_049240	HSP beta-1	7.82	1.09E-08							
Smp_133770	Glutamine synthetase bacteria	6.94	1.44E-21							
Smp_138070	MEG-3 (Grail) family	6.86	4.14E-08							
Smp_176110	Uncharacterized protein	6.62	4.76E-55							
Smp_188200	Uncharacterized protein	6.53	1.11E-11							
Smp_138080	MEG-3 (Grail) family	6.23	3.05E-07							
Smp_040680	Cytoplasmic dynein light chain	5.41	2.05E-17							
Smp_072460	Phosphomevalonate kinase	5.38	8.49E-25							
Smp_180190	Uncharacterized protein	5.33	2.77E-95							
Smp_079960	Tubulin beta chain	5.01	1.86E-08							
Smp_160170	Uncharacterized protein	4.97	5.57E-18							
Smp_067890*	Proteasome subunit alpha type	2.06	7.99E-18							
Smp_025800*	Proteasome subunit beta type	1.57	5.83E-12							

Table 4. Developmental stage expression of the top 20 upregulated genes and the ten qPCR genes after exposure to CFZ for 24 h (Continued)

				ME	MG	ML	MS	MC	MA	MF
Smp_119310*	26S Proteasome regulatory subunit	1.73	3.51E-17			▓	▓		▓	
Smp_102240*	Upf3 regulator of nonsense transcripts-like protein	2.05	6.89E-20							
Smp_052870*	26S Proteasome non-ATPase regulatory subunit	1.90	4.03E-15	▓		▓			▓	
Smp_072340*	26S Protease regulatory subunit 6b	2.12	7.61E-09	▓		▓				
Smp_171150*	Shk1 kinase-binding protein	2.54	2.68E-19						▓	
Smp_123260*	Ubiquitin 1 protein	4.11	3.48E-15						▓	

[a]Key (taken from the terms used in the NCBI EST database): ME, egg; MG, germball (sporocyst); ML, miracidium; MS, schistosomulum; MC, cercaria; MA, mixed-sex adult; MF, adult female. Empty cells indicate that no EST sequence data were found.
* indicates the ten qPCR-validated genes.

5. Discussion

Schistosomiasis remains one of the most prevalent neglected tropical diseases with over 200 million people infected worldwide and 700 million people at risk of infection [2]. Effective control is challenging in the absence of vaccines. The current reliance on just one drug (PZQ) [17], the high rates of reinfection, and concerns regarding the emergence and establishment of PZQ-resistant strains emphasize the need to identify new drugs and drug targets for schistosomiasis [18].

In this study, I investigated the transcriptomic changes in adult male *S. mansoni* after *in vitro* exposure to CFZ as compared to a second proteasome inhibitor, BTZ, and the non-proteasome inhibitor, OXO, which is an experimental drug for treatment of Friedreich's Ataxia [73]. My thesis research is part of a larger project to understand whether the proteasome is a useful drug target for treatment of schistosomiasis based on the precedent that it has been validated as such for other parasitic diseases, namely malaria and leishmaniasis [59; 67; 68], and our prior

demonstration that proteasome inhibitors kill schistosomes [63]. Understanding the underlying changes in gene expression after inhibition of the proteasome could also point to new targets for drug treatment.

The genome of *S. mansoni* was first sequenced in 2009 [89] and its annotation was improved in 2012 [90]. These developments heralded a new age in the systematic identification and characterization of genes in all aspects of schistosome biology and parasitism, and in our case, in relation to possible new drug targets. In this context, one point to note is that we found it necessary to manually reannotate some of the top 300 genes that had been up and downregulated after exposure to CFZ. About 39% and 44% of the top 300 up and downregulated genes, respectively, had been originally annotated as hypothetical or uncharacterized. After manual BLAST analysis the respective percentages were decreased to 12% and 9%.

The 10 most upregulated genes following treatment with CFZ at 24 h are listed in **Table 2**. At the very top is a Major Egg Antigen (Smp_185680), which, based on KEGG pathway analysis, is involved in Genetic Information Processing and defined to have heat shock-associated properties. A second Major Egg Antigen (Smp_049300) appears at position 5 in **Table 2**. These Major Egg Antigen proteins are 99.36% identical and provoke a Th2-type immune response that in mice and humans results from secretion of proteins by *S. mansoni* eggs [91-93]. Despite its name, Major Egg Antigen is not egg-specific but is found in all developmental stages of the parasite (**Table 4** and [94]).

Apart from the two Major Egg Antigens, there were five HSPs: Smp_049250, Smp_106930, Smp_048050, Smp_049230 and Smp_049240, that were significantly upregulated following treatment with CFZ (**Table 2**; **Suppl. Table 1**). HSPs are upregulated in cells in response to stress and act as chaperones that bind proteins and modulate their conformation [95]. HSPs are

categorized into six different families of protein chaperones based on their molecular function and mass: the small HSP20/alpha-crystallin family, the HSP40 J-protein family, and the large HSP60, HSP70, HSP90 and HSP100 families [96].

HSPs like HSP40, HSP60, HSP70 and HSP90 are expressed in parasites and known to modulate the host immune response [97-99]. Recent western blot analysis revealed that HSP40 and HSP90a are overexpressed in *S. japonicum* eggs compared to other life stages. This finding supports the involvement of HSPs as host immune response modulators, as is also the case for many other proteins that are secreted from eggs [100]. HSP70 (Smp_106930) is a strong immunogen in *S. mansoni*-infected baboons [101] and also has potential as a diagnostic marker of infection in humans [102].

An elevation in the expression of HSPs after treatment with CFZ is consistent with data reported for BTZ by our lab ([71]; El-Sakkary et al., 2021, *manuscript in prep.*). Our combined data are also consistent with the cancer cell literature where it is well-established that HSP transcription is elevated in response to proteasome inhibitor treatment. This upregulation is as part of the cell's response in managing the resulting increase in unfolded proteins [71; 103-105]. HSPs are proven drug targets: an HSP90 inhibitor exhibits antitumor activity in xenograft models of breast and prostate cancer [106; 107] and HSP70 is a putative target for tumor therapy [108; 109].

Apart from the 10 most upregulated genes expressed following treatment with CFZ, genes associated with proteasome function were also upregulated, including ubiquitin- and ubiquitination-associated genes which make up the 13% of those genes that are involved in Genetic Information Processing (**Fig. 5B, Suppl. Table 1**). Among these genes are multiple proteasomal subunits, including those comprising the 20S core α subunits (Smp_067890, Smp_092280, Smp_076230, Smp_070930, Smp_032580, and Smp_170730) and β subunits (Smp_121430,

Smp_074500, Smp_073410, and Smp_025800). Additionally, various 19S proteasome regulatory subunits were upregulated, *i.e.*, Smp_061650, Smp_085310, Smp_047740, Smp_052870, Smp_175250, Smp_058650, Smp_026630 and Smp_181380. This increase in expression of components of the proteasome as a response to its inhibition is consistent with the literature for *Drosophila* [110; 111], primary mammalian cells [112] and cancer cells [113]. An increase in proteasome expression was also reported by our lab after treatment with BTZ ([71]; El-Sakkary et al., 2021, *manuscript in prep.*). This proteasome inhibitor-mediated upregulation was not observed after treatment with the experimental Friedreich's ataxia drug inhibitor, OXO (**Table 5**), suggesting that OXO, which is eventually lethal to the parasite, operates via pathways that do not involve the proteasome. As a whole, the data suggest that inhibition of the proteasome results in compensatory *de novo* synthesis [112]. In mammalian cells, inhibition of the proteasome leads to apoptosis [114; 115], a phenomenon that has also been recently reported for *S. mansoni* by our lab [63].

Table 5. Selection of genes that were differentially upregulated by CFZ and BTZ but not by OXO

Smp ID	Description	Fold Change CFZ	Fold Change BTZ	Fold Change OXO
Smp_067890	Proteasome subunit alpha type	1.54	2.06	n.p.[a]
Smp_121430	Proteasome subunit beta type	1.98	1.54	n.p.
Smp_074500	Proteasome subunit beta 2 (T01 family)	1.89	1.55	n.p.
Smp_061650	26S proteasome subunit S9	2.02	1.57	n.p.
Smp_052870	Putative 19s proteasome non-ATPase regulatory subunit	1.90	1.55	n.p.
Smp_181380	Putative 19s proteasome non-ATPase regulatory subunit	1.53	1.53	n.p.
Smp_138060	MEG-3 (Grail) family	23.09	4.47	n.p.
Smp_138070	MEG-3 (Grail) family	6.86	4.55	n.p.
Smp_138080	MEG-3 (Grail) family	6.23	4.92	n.p.

[a]n.p.: not present in the particular dataset.

Interestingly, a family of Micro-Exon Genes-3 (MEG-3; Smp_138060, Smp_138070 and Smp_138080) was overexpressed 4 – 23-fold following treatment with CFZ and BTZ [71], but not with OXO (**Table 5**). This MEG-3 family is involved in immune evasion by the parasite [116]. When used to vaccinate mice, MEG-3.2 (Smp_138060) and a related, MEG-3.4 protein (Smp_138090), induced both humoral and cellular responses. Thus, MEG-3.2 has the potential for serological diagnosis of schistosomiasis [116]. MEGs have also been shown to induce Th1/Th2-type responses and vaccination with rSM10.3, a member of the related MEG-4 family, reduced worm and egg burdens in mice challenged with *S. mansoni* [117]. The association between

proteasome inhibition and induction of MEG-3 identified here is novel and the underlying molecular pathways will be investigated.

Among the 300 genes most downregulated after treatment with CFZ are eight genes associated with the surface tegument of the parasite (**Table 3, Suppl. Table 2**), namely, a series of "tegumental antigens" (Smp_195090, Smp_169200, Smp_195190, Smp_045010, Smp_045200; fold change: -4.85 to -14.70) and "tegumental proteins" (Smp_086530, Smp_074460; fold change: -11.42 and -4.55 respectively). The schistosome tegument is a vital protective membrane comprising two juxtaposed lipid bilayers incorporated with various proteins [118; 119]. The tegument undergoes continual turnover and is responsible for the uptake of nutrients such as glucose, and evasion of the immune response, including via the direct incorporation of host proteins [120-122]. Accordingly, downregulation of these tegumental proteins would conceivably reduce the ability of the parasite to renew proteins on its surface, thus increasing its susceptibility to immune attack. The pharmacologically targeting of the schistosome tegument that allows the immune system to eliminate the parasite from the host is a proven therapeutic approach, including for PZQ [37].

Finally, among the most downregulated genes after treatment with CFZ (as we all as BTZ and OXO [71]; El-Sakkary et al., 2021, *manuscript in prep.*) are multiple genes linked to lipid metabolism that make up part of the KEGG metabolism category (**Figure 8; Suppl. Table 2**). These genes include several steroid dehydrogenases (Smp_159600, Smp_168550, Smp_084570, Smp_178940, Smp_131430 and Smp_102190), phospholipase A (Smp_160880), lipase 1 (Smp_037780), fatty acid desaturase (Smp_132740), phosphodiesterase (Smp_153390), ATP11b phospholipid-transporting ATPase (Smp_175820), low-density lipoprotein receptor (Smp_020550), diacylglycerol O-acyltransferase 1 (Smp_158510) and dihydroceramide

desaturase (Smp_145900). As the total lipid content makes up approximately 25% of the parasite's dry body weight [123], a properly orchestrated lipid regulation is key to successful parasitism by the schistosome [124], not least in the progression of the different life-cycle stages [125], immune evasion [126] and maintenance of the parasite's tegument [127-129].

The downregulation of key lipid metabolism enzymes associated with the activity of *S. mansoni* proteasome inhibitors is consistent with a study of the rat livers in which BTZ decreased the synthesis of fatty acids, triglycerides and cholesterol [130].   Indirectly, the proteasome is responsible for degrading a number of lipid droplet proteins [131], including an ortholog of the diacylglycerol O-acyltransferase (Smp_158510) noted above [132].

Conclusion

The research presented here is part of a larger investigation by my research colleagues to characterize the proteasome as a potential drug target for schistosomiasis treatment. Using RNA-Seq, my thesis has shown that several genes and gene families are up and downregulated in *S. mansoni* after exposure to 1 µM CFZ for 24 h. These conditions induce parasite immobility and an increase in caspase activity [63], the latter of which is a common finding for proteasome inhibition in mammalian cells [133; 134]. Certain genes and gene families (*e.g.*, HSPs) were upregulated by all three drugs tested, whereas other genes, specifically, the proteasome subunits and MEG-3 proteins, were only upregulated following exposure to proteasome inhibitors. Among the most downregulated genes common to all three drugs were those associated with the tegument and lipid metabolism. The global data generated by my thesis provide a foundation to identify gene products that could be useful pharmacological targets, either independently or when combined with proteasome inhibition [135-137].

Supplementary method
1. Manual GEP analysis in Excel

Using the ROSALIND[TM] (OnRamp Bio, CA, USA) data, significantly expressed genes for different drugs and conditions were grouped in Excel according to Smp identifiers. Using gene categories and subcategories, genes were subsequently counted and separated, depending on drug treatment and incubation period.

First, gene Smp IDs that were common for different drug treatments were identified using the "FILTER" Excel function as in the following example.

FILTER I. =FILTER(A2:A301, 1-COUNTIF(C2:C301, A2:A301[EN1] [EN2]))

FILTER II. =FILTER(C2:C301, 1-COUNTIF(A2:A301, C2:C301))

Unless indicated otherwise, gene lists in columns "A" or "C" were compared using each of six possible pairings of the following treatments: BTZ 24 (24h), CFZ (24h), or OXO (24h). The number of genes common between both lists in column "A" and "C" was calculated by subtracting the result of FILTER I from FILTER II. To automate three-way comparisons in different comparative combinations, a Macro code was written in Visual Basic for Applications (VBA; Version 6.0, Microsoft, WA, USA).

2. RStudio™

     Venn Diagrams were generated in RStudio™ (2020, MA, USA) using data generated in Excel (Microsoft Excel®, 2019).

Two-way Venn Diagrams were generated as in the following example of CFZ 24 h and BTZ 24 h:

```
grid.newpage()draw.pairwise.venn(2467, 1590, 990, category = c("CFZ 24", "BTZ 24"), lty =
rep("blank",2), fill = c("red", "yellow"), alpha = rep(0.5, 2), cat.pos = c(0,0), cat.dist = rep(0.025,
2))
```

Three-way Venn Diagrams were generated as in the following example for OXO 24 h, BTZ 24 h, and CFZ 24 h:

```
rm(list=ls())

library(VennDiagram)

library(readxl)

exceldata <- read_excel(file.choose(), sheet = 1)

set1 <- na.omit(exceldata$`OXO 24h`)

set2 <- na.omit(exceldata$`BTZ 24`)

set3 <- na.omit(exceldata$`CFZ 24h`)

venn.diagram(  x = list(set1, set2, set3),

category.names = c("Set 1" , "Set 2 " , "Set 3"),

filename = 'venn_diagramm.png',  output=TRUE)
```

An example of the code used to generate a Venn diagram with the respective colors for the drug treatment is given here:

```
> grid.newpage()

> draw.triple.venn(area1 = 1590, area2 = 2467, area3 = 2946, n12 = 990, n23 = 1838, n13 =

1223,

+               n123 = 906, category = c("CFZ 24", "BTZ 24", "OXO 24"), lty = "blank",

+               fill = c("red", "yellow", " light green"))
```

3. Pie Charts

Using the RNA-Seq data our lab generated using ROSALIND™, genes for different drugs and conditions were grouped in Excel with associated Smp identifiers. The gene categories and subcategories were then counted and grouped according to drug treatment and incubation period. Each set of gene categories and subcategories was counted using Visual Basic™ (Version 6.0, Microsoft, Redmond, WA). The "COUNT" function in Excel was used to determine the number of genes in each category and the "VLOOKUP" function in Excel was used to match genes in subcategories to their associated categories. We used the data obtained for each drug condition to generate pie charts that display the proportions of genes associated with each primary and secondary KEGG pathways (including those broken out from the Genetic Info Processing portion) using Prism software (Prism version 6.04 for Windows, GraphPad Software, CA, USA).

References

Gryseels, B., K. Polman, J. Clerinx, and L. Kestens. "Human Schistosomiasis." *Lancet* 368.9541 (2006): 1106-18. Print.

Chitsulo, L., D. Engels, A. Montresor, and L. Savioli. "The Global Status of Schistosomiasis and Its Control." *Acta Trop* 77.1 (2000): 41-51. Print.

Hotez, Peter J., Ashish Damania, and Mohsen Naghavi. "Blue Marble Health and the Global Burden of Disease Study 2013." *PLOS Neglected Tropical Diseases* 10.10 (2016): e0004744. Print.

Colley, Daniel G., Amaya L. Bustinduy, W. Evan Secor, and Charles H. King. "Human Schistosomiasis." *Lancet (London, England)* 383.9936 (2014): 2253-64. Print.

Pearce, E. J., and A. S. MacDonald. "The Immunobiology of Schistosomiasis." *Nat Rev Immunol* 2.7 (2002): 499-511. Print.

CDC. "Schistosomiasis " Biology. (n.d.). . Web. February 13 2021.

Bais, Swarna, and Robert M. Greenberg. "Trp Channels as Potential Targets for Antischistosomals." *International journal for parasitology. Drugs and drug resistance* 8.3 (2018): 511-17. Print.

Burke, M. L., M. K. Jones, G. N. Gobert, Y. S. Li, M. K. Ellis, and D. P. McManus. "Immunopathogenesis of Human Schistosomiasis." *Parasite Immunol* 31.4 (2009): 163-76. Print.

de Jesus, Amelia Ribeiro, Angela Silva, Luciana B. Santana, Andrea Magalhães, Adriana Almeida de Jesus, Roque Pacheco de Almeida, Marco A. V. Rêgo, Marcelo N. Burattini, Edward J. Pearce, and Edgar M. Carvalho. "Clinical and Immunologic Evaluation of 31 Patients with Acute Schistosomiasis Mansoni." *The Journal of Infectious Diseases* 185.1 (2002): 98-105. Print.

Pearce, E J, P Caspar, J M Grzych, F A Lewis, and A Sher. "Downregulation of Th1 Cytokine Production Accompanies Induction of Th2 Responses by a Parasitic Helminth, Schistosoma Mansoni." *Journal of Experimental Medicine* 173.1 (1991): 159-66. Print.

McManus, Donald P., David W. Dunne, Moussa Sacko, Jürg Utzinger, Birgitte J. Vennervald, and Xiao-Nong Zhou. "Schistosomiasis." *Nature Reviews Disease Primers* 4.1 (2018): 13. Print.

Dunne, D. W., and E. J. Pearce. "Immunology of Hepatosplenic Schistosomiasis Mansoni: A Human Perspective." *Microbes Infect* 1.7 (1999): 553-60. Print.

Wilson, M. S., M. M. Mentink-Kane, J. T. Pesce, T. R. Ramalingam, R. Thompson, and T. A. Wynn. "Immunopathology of Schistosomiasis." *Immunol Cell Biol* 85.2 (2007): 148-54. Print.

Fallon, P. G. "Immunopathology of Schistosomiasis: A Cautionary Tale of Mice and Men." *Immunol Today* 21.1 (2000): 29-35. Print.

Schramm, G., A. Gronow, J. Knobloch, V. Wippersteg, C. G. Grevelding, J. Galle, H. Fuller, R. G. Stanley, P. L. Chiodini, H. Haas, and M. J. Doenhoff. "Ipse/Alpha-1: A Major Immunogenic Component Secreted from Schistosoma Mansoni Eggs." *Mol Biochem Parasitol* 147.1 (2006): 9-19. Print.

Schramm, Gabriele, Katja Mohrs, Maren Wodrich, Michael J. Doenhoff, Edward J. Pearce, Helmut Haas, and Markus Mohrs. "Cutting Edge: Ipse/Alpha-1, a Glycoprotein from <Em>Schistosoma Mansoni</Em> Eggs, Induces Ige-Dependent, Antigen-Independent Il-4 Production by Murine Basophils in Vivo." *The Journal of Immunology* 178.10 (2007): 6023-27. Print.

Doenhoff, M. J., D. Cioli, and J. Utzinger. "Praziquantel: Mechanisms of Action, Resistance and New Derivatives for Schistosomiasis." *Curr Opin Infect Dis* 21.6 (2008): 659-67. Print.

Cioli, Donato, and Livia Pica-Mattoccia. "Praziquantel." *Parasitology Research* 90.1 (2003): S3-S9. Print.

Knuhr, Katrin, Kristina Langhans, Sandra Nyenhuis, Kerstin Viertmann, Anna M. Overgaard Kildemoes, Michael J. Doenhoff, Helmut Haas, and Gabriele Schramm. "Schistosoma Mansoni Egg-Released Ipse/Alpha-1 Dampens Inflammatory Cytokine Responses Via Basophil Interleukin (Il)-4 and Il-13." *Frontiers in Immunology* 9.2293 (2018). Print.

Dunne, D. W., F. M. Jones, and M. J. Doenhoff. "The Purification, Characterization, Serological Activity and Hepatotoxic Properties of Two Cationic Glycoproteins (Alpha 1 and Omega 1) from Schistosoma Mansoni Eggs." *Parasitology* 103 Pt 2 (1991): 225-36. Print.

Steinfelder, S., J. F. Andersen, J. L. Cannons, C. G. Feng, M. Joshi, D. Dwyer, P. Caspar, P. L. Schwartzberg, A. Sher, and D. Jankovic. "The Major Component in Schistosome Eggs Responsible for Conditioning Dendritic Cells for Th2 Polarization Is a T2 Ribonuclease (Omega-1)." *J Exp Med* 206.8 (2009): 1681-90. Print.

Everts, B., G. Perona-Wright, H. H. Smits, C. H. Hokke, A. J. van der Ham, C. M. Fitzsimmons, M. J. Doenhoff, J. van der Bosch, K. Mohrs, H. Haas, M. Mohrs, M. Yazdanbakhsh, and G. Schramm. "Omega-1, a Glycoprotein Secreted by Schistosoma Mansoni Eggs, Drives Th2 Responses." *J Exp Med* 206.8 (2009): 1673-80. Print.

Caldas, Iramaya Rodrigues, Ana Carolina Campi-Azevedo, Lucia Fraga Alves Oliveira, Alda Maria Soares Silveira, Rodrigo C. Oliveira, and Giovanni Gazzinelli. "Human Schistosomiasis Mansoni: Immune Responses During Acute and Chronic Phases of the Infection." *Acta Tropica* 108.2 (2008): 109-17. Print.

Gryseels, B., and A. M. Polderman. "Morbidity, Due to Schistosomiasis Mansoni, and Its Control in Subsaharan Africa." *Parasitology Today* 7.9 (1991): 244-48. Print.

Mostafa, M. H., S. A. Sheweita, and P. J. O'Connor. "Relationship between Schistosomiasis and Bladder Cancer." *Clin Microbiol Rev* 12.1 (1999): 97-111. Print.

Iduh, MU, and UH Bwari. "Urogenital Schistosomiasis Study in a Rural Community, North West Nigeria." *Asian Journal of Research in Infectious Diseases* (2021): 12-20. Print.

Cheever, Allen W, A Kamel, Anwar M Elwi, James E Mosimann, Ray Danner, and John E Sippel. "Schistosoma Mansoni and S. Haematobium Infections in Egypt." *The American journal of tropical medicine and hygiene* 27.1 (1978): 55-75. Print.

World Health, Organization. *Female Genital Schistosomiasis: A Pocket Atlas for Clinical Health-Care Professionals*. Geneva: World Health Organization, 2015. Print.

Kjetland, E. F., P. D. Ndhlovu, E. Gomo, T. Mduluza, N. Midzi, L. Gwanzura, P. R. Mason, L. Sandvik, H. Friis, and S. G. Gundersen. "Association between Genital Schistosomiasis and Hiv in Rural Zimbabwean Women." *Aids* 20.4 (2006): 593-600. Print.

Mostafa, M. H., S. A. Sheweita, and P. J. O'Connor. "Relationship between Schistosomiasis and Bladder Cancer." *Clinical microbiology reviews* 12.1 (1999): 97-111. Print.

Humans., IARC Working Group on the Evaluation of Carcinogenic Risks to. "Schistosomes, Liver Flukes and Helicobacter Pylori. Iarc Working Group on the Evaluation of Carcinogenic Risks to Humans. Lyon, 7-14 June 1994." *Lyon (FR): International Agency for Research on Cancer* 61 (1994): 1-241. Print.

Bedwani, R., E. Renganathan, F. El Kwhsky, C. Braga, H. H. Abu Seif, T. Abul Azm, A. Zaki, S. Franceschi, P. Boffetta, and C. La Vecchia. "Schistosomiasis and the Risk of Bladder Cancer in Alexandria, Egypt." *Br J Cancer* 77.7 (1998): 1186-9. Print.

Groll, E. "Praziquantel." *Adv Pharmacol Chemother* 20 (1984): 219-38. Print.

Utzinger, Jürg, Eliézer K. N'goran, Amani N'dri, Christian Lengeler, and Marcel Tanner. "Efficacy of Praziquantel against Schistosoma Mansoni with Particular Consideration for Intensity of Infection." *Tropical Medicine & International Health* 5.11 (2000): 771-78. Print.

Fallon, P. G., and M. J. Doenhoff. "Drug-Resistant Schistosomiasis: Resistance to Praziquantel and Oxamniquine Induced in Schistosoma Mansoni in Mice Is Drug Specific." *Am J Trop Med Hyg* 51.1 (1994): 83-8. Print.

Pax, R., J. L. Bennett, and R. Fetterer. "A Benzodiazepine Derivative and Praziquantel: Effects on Musculature of Schistosoma Mansoni and Schistosoma Japonicum." *Naunyn-Schmiedeberg's Archives of Pharmacology* 304.3 (1978): 309-15. Print.

Becker, B., H. Mehlhorn, P. Andrews, H. Thomas, and J. Eckert. "Light and Electron Microscopic Studies on the Effect of Praziquantel on Schistosoma Mansoni, Dicrocoelium Dendriticum, and Fasciola Hepatica (Trematoda) in Vitro." *Z Parasitenkd* 63.2 (1980): 113-28. Print.

Oliveira, Claudineide, Rosimeire De Oliveira, Tarsila Frezza, Vera Rehder, and Silmara Allegretti. "Tegument of Schistosoma Mansoni as a as a Therapeutic Target." 2013. 151-77. Print.

Southgate, V. R. "Schistosomiasis in the Senegal River Basin: Before and after the Construction of the Dams at Diama, Senegal and Manantali, Mali and Future Prospects." *J Helminthol* 71.2 (1997): 125-32. Print.

Stelma, F. F., I. Talla, S. Sow, A. Kongs, M. Niang, K. Polman, A. M. Deelder, and B. Gryseels. "Efficacy and Side Effects of Praziquantel in an Epidemic Focus of Schistosoma Mansoni." *Am J Trop Med Hyg* 53.2 (1995): 167-70. Print.

Mitch, W. E., and A. L. Goldberg. "Mechanisms of Muscle Wasting. The Role of the Ubiquitin-Proteasome Pathway." *N Engl J Med* 335.25 (1996): 1897-905. Print.

Xiao, S. H., B. A. Catto, and L. T. Webster, Jr. "Effects of Praziquantel on Different Developmental Stages of Schistosoma Mansoni in Vitro and in Vivo." *J Infect Dis* 151.6 (1985): 1130-7. Print.

Kasinathan, Ravi S., William M. Morgan, and Robert M. Greenberg. "Schistosoma Mansoni Express Higher Levels of Multidrug Resistance-Associated Protein 1 (Smmrp1) in Juvenile Worms and in Response to Praziquantel." *Molecular and biochemical parasitology* 173.1 (2010): 25-31. Print.

Bhattacharyya, S., H. Yu, C. Mim, and A. Matouschek. "Regulated Protein Turnover: Snapshots of the Proteasome in Action." *Nat Rev Mol Cell Biol* 15.2 (2014): 122-33. Print.

Bedford, L., S. Paine, P. W. Sheppard, R. J. Mayer, and J. Roelofs. "Assembly, Structure, and Function of the 26s Proteasome." *Trends Cell Biol* 20.7 (2010): 391-401. Print.

Groll, M., W. Heinemeyer, S. Jäger, T. Ullrich, M. Bochtler, D. H. Wolf, and R. Huber. "The Catalytic Sites of 20s Proteasomes and Their Role in Subunit Maturation: A Mutational and Crystallographic Study." *Proceedings of the National Academy of Sciences of the United States of America* 96.20 (1999): 10976-83. Print.

Bochtler, M., L. Ditzel, M. Groll, C. Hartmann, and R. Huber. "The Proteasome." *Annu Rev Biophys Biomol Struct* 28 (1999): 295-317. Print.

Ciechanover, A., A. Orian, and A. L. Schwartz. "Ubiquitin-Mediated Proteolysis: Biological Regulation Via Destruction." *Bioessays* 22.5 (2000): 442-51. Print.

Landis-Piwowar, Kristin R., Vesna Milacic, Di Chen, Huanjie Yang, Yunfeng Zhao, Tak Hang Chan, Bing Yan, and Q. Ping Dou. "The Proteasome as a Potential Target for Novel Anticancer Drugs and Chemosensitizers." *Drug Resistance Updates* 9.6 (2006): 263-73. Print.

Orlowski, R. Z. "The Ubiquitin Proteasome Pathway from Bench to Bedside." *Hematology Am Soc Hematol Educ Program* (2005): 220-5. Print.

Voorhees, P. M., E. C. Dees, B. O'Neil, and R. Z. Orlowski. "The Proteasome as a Target for Cancer Therapy." *Clin Cancer Res* 9.17 (2003): 6316-25. Print.

Lü, Shuqing, and Jianmin Wang. "The Resistance Mechanisms of Proteasome Inhibitor Bortezomib." *Biomarker research* 1.1 (2013): 13-13. Print.

Groll, M., C. R. Berkers, H. L. Ploegh, and H. Ovaa. "Crystal Structure of the Boronic Acid-Based Proteasome Inhibitor Bortezomib in Complex with the Yeast 20s Proteasome." *Structure* 14.3 (2006): 451-6. Print.

Yoo, Ji Young, Alena Cristina Jaime-Ramirez, Chelsea Bolyard, Hongsheng Dai, Tejaswini Nallanagulagari, Jeffrey Wojton, Brian S. Hurwitz, Theresa Relation, Tae Jin Lee, Michael T. Lotze, Jun-Ge Yu, Jianying Zhang, Carlo M. Croce, Jianhua Yu, Michael A. Caligiuri, Matthew Old, and Balveen Kaur. "Bortezomib Treatment Sensitizes Oncolytic Hsv-1-Treated Tumors to Nk Cell Immunotherapy." *Clinical cancer research : an official journal of the American Association for Cancer Research* 22.21 (2016): 5265-76. Print.

Frankel, Andrea, Shan Man, Peter Elliott, Julian Adams, and Robert S. Kerbel. "Lack of Multicellular Drug Resistance Observed in Human Ovarian and Prostate Carcinoma Treated with the Proteasome Inhibitor Ps-341." *Clinical Cancer Research* 6.9 (2000): 3719-28. Print.

Papandreou, Christos N, Danai D Daliani, Darrell Nix, Hong Yang, Timothy Madden, Xuemei Wang, Christine S Pien, Randall E Millikan, Shi-Ming Tu, and Lance Pagliaro. "Phase I Trial of the Proteasome Inhibitor Bortezomib in Patients with Advanced Solid Tumors with Observations in Androgen-Independent Prostate Cancer." *Journal of Clinical Oncology* 22.11 (2004): 2108-21. Print.

Steverding, Dietmar, and Xia Wang. "Trypanocidal Activity of the Proteasome Inhibitor and Anti-Cancer Drug Bortezomib." *Parasites & vectors* 2.1 (2009): 29-29. Print.

Jain, S., C. Diefenbach, J. Zain, and O. A. O'Connor. "Emerging Role of Carfilzomib in Treatment of Relapsed and Refractory Lymphoid Neoplasms and Multiple Myeloma." *Core Evid* 6 (2011): 43-57. Print.

Khare, S., A. S. Nagle, A. Biggart, Y. H. Lai, F. Liang, L. C. Davis, S. W. Barnes, C. J. Mathison, E. Myburgh, M. Y. Gao, J. R. Gillespie, X. Liu, J. L. Tan, M. Stinson, I. C. Rivera, J. Ballard, V. Yeh, T. Groessl, G. Federe, H. X. Koh, J. D. Venable, B. Bursulaya, M. Shapiro, P. K. Mishra, G. Spraggon, A. Brock, J. C. Mottram, F. S. Buckner, S. P. Rao, B. G. Wen, J. R. Walker, T. Tuntland, V. Molteni, R. J. Glynne, and F. Supek. "Proteasome Inhibition for Treatment of Leishmaniasis, Chagas Disease and Sleeping Sickness." *Nature* 537.7619 (2016): 229-33. Print.

Guo, N., and Z. Peng. "Mg132, a Proteasome Inhibitor, Induces Apoptosis in Tumor Cells." *Asia Pac J Clin Oncol* 9.1 (2013): 6-11. Print.

Groen, K., Nwcj van de Donk, Cam Stege, S. Zweegman, and I. S. Nijhof. "Carfilzomib for Relapsed and Refractory Multiple Myeloma." *Cancer management and research* 11 (2019): 2663-75. Print.

Kuhn, Deborah J, Qing Chen, Peter M Voorhees, John S Strader, Kevin D Shenk, Congcong M Sun, Susan D Demo, Mark K Bennett, Fijs WB Van Leeuwen, and Asher A Chanan-Khan. "Potent Activity of Carfilzomib, a Novel, Irreversible Inhibitor of the Ubiquitin-Proteasome Pathway, against Preclinical Models of Multiple Myeloma." *Blood, The Journal of the American Society of Hematology* 110.9 (2007): 3281-90. Print.

Bibo-Verdugo, Betsaida, Steven C Wang, Jehad Almaliti, Anh P Ta, Zhenze Jiang, Derek A Wong, Christopher B Lietz, Brian M Suzuki, Nelly El-Sakkary, and Vivian Hook. "The Proteasome as a Drug Target in the Metazoan Pathogen, Schistosoma Mansoni." *ACS infectious diseases* 5.10 (2019): 1802-12. Print.

Karademir, Betul, Gulce Sari, Ayse Tarbin Jannuzzi, Sravani Musunuri, Grzegorz Wicher, Tilman Grune, Jia Mi, Husniye Hacioglu-Bay, Karin Forsberg-Nilsson, and Jonas Bergquist. "Proteomic Approach for Understanding Milder Neurotoxicity of Carfilzomib against Bortezomib." *Scientific reports* 8.1 (2018): 1-13. Print.

Gu, Juan J, Francisco J Hernandez-Ilizaliturri, Gregory P Kaufman, Natalie M Czuczman, Cory Mavis, Joseph J Skitzki, and Myron S Czuczman. "The Novel Proteasome Inhibitor Carfilzomib Induces Cell Cycle Arrest, Apoptosis and Potentiates the Anti-Tumour Activity of Chemotherapy in Rituximab-Resistant Lymphoma." *British journal of haematology* 162.5 (2013): 657-69. Print.

Tsakiri, Eleni N, Evangelos Terpos, Eleni-Dimitra Papanagnou, Efstathios Kastritis, Vincent Brieudes, Maria Halabalaki, Tina Bagratuni, Bogdan I Florea, Herman S Overkleeft, and Luca Scorrano. "Milder Degenerative Effects of Carfilzomib Vs. Bortezomib in the Drosophila Model: A Link to Clinical Adverse Events." *Scientific reports* 7.1 (2017): 1-12. Print.

Bibo-Verdugo, B., Z. Jiang, C. R. Caffrey, and A. J. O'Donoghue. "Targeting Proteasomes in Infectious Organisms to Combat Disease." *Febs j* 284.10 (2017): 1503-17. Print.

Li, Hao, Elizabeth L. Ponder, Martijn Verdoes, Kristijana H. Asbjornsdottir, Edgar Deu, Laura E. Edgington, Jeong Tae Lee, Christopher J. Kirk, Susan D. Demo, Kim C. Williamson, and Matthew Bogyo. "Validation of the Proteasome as a Therapeutic Target in Plasmodium Using an Epoxyketone Inhibitor with Parasite-Specific Toxicity." *Chemistry & biology* 19.12 (2012): 1535-45. Print.

Guerra-Sá, R., W. Castro-Borges, E. A. Evangelista, I. C. Kettelhut, and V. Rodrigues. "Schistosoma Mansoni: Functional Proteasomes Are Required for Development in the Vertebrate Host." *Exp Parasitol* 109.4 (2005): 228-36. Print.

Basch, P. F. "Cultivation of Schistosoma Mansoni in Vitro. I. Establishment of Cultures from Cercariae and Development until Pairing." *J Parasitol* 67.2 (1981): 179-85. Print.

Syed, Ali A. "The Effects of the Proteasome Inhibitor, Bortezomib, on the Profile of Gene Expression in the Flatworm Pathogen, Schistosoma Mansoni." University of California San Diego, 2021. Print.

Colley, D. G., and S. K. Wikel. "Schistosoma Mansoni: Simplified Method for the Production of Schistosomules." *Exp Parasitol* 35.1 (1974): 44-51. Print.

Lynch, D. R., J. Farmer, L. Hauser, I. A. Blair, Q. Q. Wang, C. Mesaros, N. Snyder, S. Boesch, M. Chin, M. B. Delatycki, P. Giunti, A. Goldsberry, C. Hoyle, M. G. McBride, W. Nachbauer, M. O'Grady, S. Perlman, S. H. Subramony, G. R. Wilmot, T. Zesiewicz, and C. Meyer. "Safety, Pharmacodynamics, and Potential Benefit of Omaveloxolone in Friedreich Ataxia." *Ann Clin Transl Neurol* 6.1 (2019): 15-26. Print.

Caffrey, Conor. "Plos Neglected Tropical Diseases Issue Image | Vol. 3(7) July 2009." *PLOS Neglected Tropical Diseases* 3.7 (2009): ev03.i07. Print.

Lu, Zhigang, Florian Sessler, Nancy Holroyd, Steffen Hahnel, Thomas Quack, Matthew Berriman, and Christoph G. Grevelding. "A Gene Expression Atlas of Adult Schistosoma Mansoni and Their Gonads." *Scientific data* 4 (2017): 170118-18. Print.

Luo, Weijun, Michael S Friedman, Kerby Shedden, Kurt D Hankenson, and Peter J Woolf. "Gage: Generally Applicable Gene Set Enrichment for Pathway Analysis." *BMC bioinformatics* 10.1 (2009): 1-17. Print.

Brechtmann, Felix, Christian Mertes, Agnė Matusevičiūtė, Vicente A Yépez, Žiga Avsec, Maximilian Herzog, Daniel M Bader, Holger Prokisch, and Julien Gagneur. "Outrider: A Statistical Method for Detecting Aberrantly Expressed Genes in Rna Sequencing Data." *The American Journal of Human Genetics* 103.6 (2018): 907-17. Print.

Van der Laan, Mark, Katherine Pollard, and Jennifer Bryan. "A New Partitioning around Medoids Algorithm." *Journal of Statistical Computation and Simulation* 73.8 (2003): 575-84. Print.

"Homer Software and Data Download." *http://homer.ucsd.edu/homer/* Web. February 4, 2021.

"Protein Blast: Search Protein Databases Using a Protein Query.". *https://blast.ncbi.nlm.nih.gov/Blast.cgi?PAGE=Proteins*. Web.

Consortium, The UniProt. "Uniprot: The Universal Protein Knowledgebase in 2021." *Nucleic Acids Research* 49.D1 (2020): D480-D89. Print.

Kanehisa, M., and S. Goto. "Kegg: Kyoto Encyclopedia of Genes and Genomes." *Nucleic Acids Res* 28.1 (2000): 27-30. Print.

Koetsier, Giron, and Eric Cantor. "A Practical Guide to Analyzing Nucleic Acid Concentration and Purity with Microvolume Spectrophotometers." *New England Biolabs Inc* (2019). Print.

Nolan, T., R. E. Hands, and S. A. Bustin. "Quantification of Mrna Using Real-Time Rt-Pcr." *Nat Protoc* 1.3 (2006): 1559-82. Print.

"Primer Designing Tool.". *https://www.ncbi.nlm.nih.gov/tools/primer-blast/* Web. March 14, 2021.

Roberts, Adam, Cole Trapnell, Julie Donaghey, John L. Rinn, and Lior Pachter. "Improving Rna-Seq Expression Estimates by Correcting for Fragment Bias." *Genome Biology* 12.3 (2011): R22. Print.

Livak, K. J., and T. D. Schmittgen. "Analysis of Relative Gene Expression Data Using Real-Time Quantitative Pcr and the 2(-Delta Delta C(T)) Method." *Methods* 25.4 (2001): 402-8. Print.

Silva, Larissa Lopes, Marina Marcet-Houben, Laila Alves Nahum, Adhemar Zerlotini, Toni Gabaldón, and Guilherme Oliveira. "The Schistosoma Mansoni Phylome: Using Evolutionary Genomics to Gain Insight into a Parasite's Biology." *BMC Genomics* 13.1 (2012): 617. Print.

Berriman, Matthew, Brian J. Haas, Philip T. LoVerde, R. Alan Wilson, Gary P. Dillon, Gustavo C. Cerqueira, Susan T. Mashiyama, Bissan Al-Lazikani, Luiza F. Andrade, Peter D. Ashton, Martin A. Aslett, Daniella C. Bartholomeu, Gaelle Blandin, Conor R. Caffrey, Avril Coghlan, Richard Coulson, Tim A. Day, Art Delcher, Ricardo DeMarco, Appolinaire Djikeng, Tina Eyre, John A. Gamble, Elodie Ghedin, Yong Gu, Christiane Hertz-Fowler, Hirohisha Hirai, Yuriko Hirai, Robin Houston, Alasdair Ivens, David A. Johnston, Daniela Lacerda, Camila D. Macedo, Paul McVeigh, Zemin Ning, Guilherme Oliveira, John P. Overington, Julian Parkhill, Mihaela Pertea, Raymond J. Pierce, Anna V. Protasio, Michael A. Quail, Marie-Adèle Rajandream, Jane Rogers, Mohammed Sajid, Steven L. Salzberg, Mario Stanke, Adrian R. Tivey, Owen White, David L. Williams, Jennifer Wortman, Wenjie Wu, Mostafa Zamanian, Adhemar Zerlotini, Claire M. Fraser-Liggett, Barclay G. Barrell, and Najib M. El-Sayed. "The Genome of the Blood Fluke Schistosoma Mansoni." *Nature* 460.7253 (2009): 352-58. Print.

Protasio, Anna V, Isheng J Tsai, Anne Babbage, Sarah Nichol, Martin Hunt, Martin A Aslett, Nishadi De Silva, Giles S Velarde, Tim JC Anderson, and Richard C Clark. "A Systematically Improved High Quality Genome and Transcriptome of the Human Blood Fluke Schistosoma Mansoni." *PLoS Negl Trop Dis* 6.1 (2012): e1455. Print.

Okano, M., A. R. Satoskar, K. Nishizaki, M. Abe, and D. A. Harn, Jr. "Induction of Th2 Responses and Ige Is Largely Due to Carbohydrates Functioning as Adjuvants on Schistosoma Mansoni Egg Antigens." *J Immunol* 163.12 (1999): 6712-7. Print.

Yang, J., J. Zhao, Y. Yang, L. Zhang, X. Yang, X. Zhu, M. Ji, N. Sun, and C. Su. "Schistosoma Japonicum Egg Antigens Stimulate Cd4 Cd25 T Cells and Modulate Airway Inflammation in a Murine Model of Asthma." *Immunology* 120.1 (2007): 8-18. Print.

Grzych, Jean-Marie, EDWARD Pearce, ALLEN Cheever, ZULEICA A Caulada, PATRICIA Caspar, SARA Heiny, FRED Lewis, and ALAN Sher. "Egg Deposition Is the Major Stimulus for the Production of Th2 Cytokines in Murine Schistosomiasis Mansoni." *The Journal of Immunology* 146.4 (1991): 1322-27. Print.

Nene, V., D. W. Dunne, K. S. Johnson, D. W. Taylor, and J. S. Cordingley. "Sequence and Expression of a Major Egg Antigen from Schistosoma Mansoni. Homologies to Heat Shock Proteins and Alpha-Crystallins." *Mol Biochem Parasitol* 21.2 (1986): 179-88. Print.
Sharp, F. R., S. M. Massa, and R. A. Swanson. "Heat-Shock Protein Protection." *Trends Neurosci* 22.3 (1999): 97-9. Print.

Jing, Xiao-Yang, and Feng-Min Li. "Identifying Heat Shock Protein Families from Imbalanced Data by Using Combined Features." *Computational and mathematical methods in medicine* 2020 (2020). Print.

Brandau, S., A. Dresel, and J. Clos. "High Constitutive Levels of Heat-Shock Proteins in Human-Pathogenic Parasites of the Genus Leishmania." *Biochem J* 310 (Pt 1).Pt 1 (1995): 225-32. Print.

Maresca, B., and G. S. Kobayashi. "Hsp70 in Parasites: As an Inducible Protective Protein and as an Antigen." *Experientia* 50.11-12 (1994): 1067-74. Print.

Younis, Abuelhassan Elshazly, Frank Geisinger, Irene Ajonina-Ekoti, Hanns Soblik, Hanno Steen, Makedonka Mitreva, Klaus D Erttmann, Markus Perbandt, Eva Liebau, and Norbert W Brattig. "Stage-Specific Excretory–Secretory Small Heat Shock Proteins from the Parasitic Nematode Strongyloides Ratti–Putative Links to Host's Intestinal Mucosal Defense System." *The FEBS journal* 278.18 (2011): 3319-36. Print.

Xu, Zhipeng, Minjun Ji, Chen Li, Xiaofeng Du, Wei Hu, Donald Peter McManus, and Hong You. "A Biological and Immunological Characterization of Schistosoma Japonicum Heat Shock Proteins 40 and 90α." *International journal of molecular sciences* 21.11 (2020): 4034. Print.

Kanamura, Herminia Y, Kathy Hancock, Vanderlei Rodrigues, and Raymond T Damian. "Schistosoma Mansoni Heat Shock Protein 70 Elicits an Early Humoral Immune Response in S. Mansoni Infected Baboons." *Memorias do Instituto Oswaldo Cruz* 97.5 (2002): 711-16. Print.

Moser, Doris, Ogobara Doumbo, and Mo-Quen Klinkert. "The Humoral Response to Heat Shock Protein 70 in Human and Murine Schistosomiasis Mansoni." *Parasite immunology* 12.4-5 (1990): 341-52. Print.

Rappa, Francesca, Felicia Farina, Giovanni Zummo, Sabrina David, Claudia Campanella, Francesco Carini, Giovanni Tomasello, Provvidenza Damiani, Francesco Cappello, and Everly Conway De Macario. "Hsp-Molecular Chaperones in Cancer Biogenesis and Tumor Therapy: An Overview." *Anticancer research* 32.12 (2012): 5139-50. Print.

Radons, Jürgen. "The Human Hsp70 Family of Chaperones: Where Do We Stand?" *Cell Stress and Chaperones* 21.3 (2016): 379-404. Print.

Bonora, Massimo, and Paolo Pinton. "The Mitochondrial Permeability Transition Pore and Cancer: Molecular Mechanisms Involved in Cell Death." *Frontiers in oncology* 4 (2014): 302. Print.

Basso, Andrea D, David B Solit, Pamela N Munster, and Neal Rosen. "Ansamycin Antibiotics Inhibit Akt Activation and Cyclin D Expression in Breast Cancer Cells That Overexpress Her2." *Oncogene* 21.8 (2002): 1159-66. Print.

Solit, David B, Fuzhong F Zheng, Maria Drobnjak, Pamela N Münster, Brian Higgins, David Verbel, Glenn Heller, William Tong, Carlos Cordon-Cardo, and David B Agus. "17-Allylamino-17-Demethoxygeldanamycin Induces the Degradation of Androgen Receptor and Her-2/Neu and Inhibits the Growth of Prostate Cancer Xenografts." *Clinical cancer research* 8.5 (2002): 986-93. Print.

Rohde, Mikkel, Mads Daugaard, Mette Hartvig Jensen, Kristian Helin, Jesper Nylandsted, and Marja Jäättelä. "Members of the Heat-Shock Protein 70 Family Promote Cancer Cell Growth by Distinct Mechanisms." *Genes & development* 19.5 (2005): 570-82. Print.

Ciocca, Daniel R, Gary M Clark, Atul K Tandon, Suzanne AW Fuqua, William J Welch, and William L McGuire. "Heat Shock Protein Hsp70 in Patients with Axillary Lymph Node-Negative Breast Cancer: Prognostic Implications." *JNCI: Journal of the National Cancer Institute* 85.7 (1993): 570-74. Print.

Wójcik, Cezary, and George N. DeMartino. "Analysis of Drosophila 26 S Proteasome Using Rna Interference*." *Journal of Biological Chemistry* 277.8 (2002): 6188-97. Print.

Lundgren, Josefin, Patrick Masson, Zahra Mirzaei, and Patrick Young. "Identification and Characterization of a Drosophila Proteasome Regulatory Network." *Molecular and cellular biology* 25.11 (2005): 4662-75. Print.

Meiners, Silke, Dirk Heyken, Andrea Weller, Antje Ludwig, Karl Stangl, Peter- M. Kloetzel, and Elke Krüger. "Inhibition of Proteasome Activity Induces Concerted Expression of Proteasome Genes and De Novo Formation of Mammalian Proteasomes*." *Journal of Biological Chemistry* 278.24 (2003): 21517-25. Print.

Edwards, Claire M, Seint T Lwin, Jessica A Fowler, Babatunde O Oyajobi, Junling Zhuang, Andreia L Bates, and Gregory R Mundy. "Myeloma Cells Exhibit an Increase in Proteasome Activity and an Enhanced Response to Proteasome Inhibition in the Bone Marrow Microenvironment in Vivo." *American journal of hematology* 84.5 (2009): 268-72. Print.

Chowdary, Dondapati R, James J Dermody, Krishna K Jha, and Harvey L Ozer. "Accumulation of P53 in a Mutant Cell Line Defective in the Ubiquitin Pathway." *Molecular and cellular biology* 14.3 (1994): 1997. Print.

Maki, Carl G, Jon M Huibregtse, and Peter M Howley. "In Vivo Ubiquitination and Proteasome-Mediated Degradation of P53." *Cancer research* 56.11 (1996): 2649-54. Print.

Mambelli, FS, BC Figueiredo, SB Morais, NRG Assis, CT Fonseca, and SC Oliveira. "Recombinant Micro-Exon Gene 3 (Meg-3) Antigens from Schistosoma Mansoni Failed to Induce Protection against Infection but Show Potential for Serological Diagnosis." *Acta tropica* 204 (2020): 105356. Print.

Martins, V. P., S. B. Morais, C. S. Pinheiro, N. R. Assis, B. C. Figueiredo, N. D. Ricci, J. Alves-Silva, M. V. Caliari, and S. C. Oliveira. "Sm10.3, a Member of the Micro-Exon Gene 4 (Meg-4) Family, Induces Erythrocyte Agglutination in Vitro and Partially Protects Vaccinated Mice against Schistosoma Mansoni Infection." *PLoS Negl Trop Dis* 8.3 (2014): e2750. Print.

Hockley, DJ. "Ultrastructure of the Tegument of Schistosoma." *Advances in parasitology* 11 (1973): 233-305. Print.

Van Hellemond, Jaap J., Kim Retra, Jos F. H. M. Brouwers, Bas W. M. van Balkom, Maria Yazdanbakhsh, Charles B. Shoemaker, and Aloysius G. M. Tielens. "Functions of the Tegument of Schistosomes: Clues from the Proteome and Lipidome." *International Journal for Parasitology* 36.6 (2006): 691-99. Print.

ABATH, FREDERICO GC, and ROBERTO C WERKHAUSER. "The Tegument of Schistosoma Mansoni: Functional and Immunological Features." *Parasite immunology* 18.1 (1996): 15-20. Print.

PEARCE, EDWARD J, PAUL F BASCH, and ALAN SHER. "Evidence That the Reduced Surface Antigenicity of Developing Schistosoma Mansoni Schistosomula Is Due to Antigen Shedding Rather Than Host Molecule Acquisition." *Parasite immunology* 8.1 (1986): 79-94. Print.

Rogers, Rick A, Richard M Jack, and Stephen T Furlong. "Lipid and Membrane Protein Transfer from Human Neutrophils to Schistosomes Is Mediated by Ligand Binding." *Journal of cell science* 106.2 (1993): 485-91. Print.

Skelly, P. J., A. A. Da'dara, X. H. Li, W. Castro-Borges, and R. A. Wilson. "Schistosome Feeding and Regurgitation." *PLoS Pathog* 10.8 (2014): e1004246. Print.

Giera, M., M. M. M. Kaisar, R. J. E. Derks, E. Steenvoorden, Y. C. M. Kruize, C. H. Hokke, M. Yazdanbakhsh, and B. Everts. "The Schistosoma Mansoni Lipidome: Leads for Immunomodulation." *Anal Chim Acta* 1037 (2018): 107-18. Print.

Payares, G., D. J. McLaren, W. H. Evans, and S. R. Smithers. "Changes in the Surface Antigen Profile of Schistosoma Mansoni During Maturation from Cercaria to Adult Worm." *Parasitology* 91 (Pt 1) (1985): 83-99. Print.

Parra, J. F., R. C. França, J. R. Kusel, M. V. Gomez, E. A. Figueiredo, and T. A. Mota-Santos. "Schistosoma Mansoni: Phospholipid Methylation and the Escape of Schistosomula from in Vitro Cytotoxic Reaction." *Mol Biochem Parasitol* 21.2 (1986): 151-9. Print.

Wu, Junfang, Wenxin Xu, Zhenping Ming, Huifen Dong, Huiru Tang, and Yulan Wang. "Metabolic Changes Reveal the Development of Schistosomiasis in Mice." *PLOS Neglected Tropical Diseases* 4.8 (2010): e807. Print.

Allan, David, Gilberto Payares, and W Howard Evans. "The Phospholipid and Fatty Acid Composition of Schistosoma Mansoni and of Its Purified Tegumental Membranes." *Molecular and biochemical parasitology* 23.2 (1987): 123-28. Print.

Brouwers, JFHM, PJ Skelly, LMG Van Golde, and AGM Tielens. "Studies on Phospholipid Turnover Argue against Sloughing of Tegumental Membranes in Adult Schistosoma Mansoni." *Parasitology* 119.3 (1999): 287-94. Print.

Oliva, Joan, Samuel W. French, Jun Li, and Fawzia Bardag-Gorce. "Proteasome Inhibitor Treatment Reduced Fatty Acid, Triacylglycerol and Cholesterol Synthesis." *Experimental and Molecular Pathology* 93.1 (2012): 26-34. Print.

Bersuker, Kirill, and James A. Olzmann. "Establishing the Lipid Droplet Proteome: Mechanisms of Lipid Droplet Protein Targeting and Degradation." *Biochimica et biophysica acta. Molecular and cell biology of lipids* 1862.10 Pt B (2017): 1166-77. Print.

Choi, K., H. Kim, H. Kang, S. Y. Lee, S. J. Lee, S. H. Back, S. H. Lee, M. S. Kim, J. E. Lee, J. Y. Park, J. Kim, S. Kim, J. H. Song, Y. Choi, S. Lee, H. J. Lee, J. H. Kim, and S. Cho. "Regulation of Diacylglycerol Acyltransferase 2 Protein Stability by Gp78-Associated Endoplasmic-Reticulum-Associated Degradation." *Febs j* 281.13 (2014): 3048-60. Print.

Concannon, C. G., B. F. Koehler, Claus Reimertz, B. M. Murphy, C. Bonner, N. Thurow, M. W. Ward, A. Villunger, A. Strasser, D. Kögel, and J. H. M. Prehn. "Apoptosis Induced by Proteasome Inhibition in Cancer Cells: Predominant Role of the P53/Puma Pathway." *Oncogene* 26.12 (2007): 1681-92. Print.

Imajoh-Ohmi, S., T. Kawaguchi, S. Sugiyama, K. Tanaka, S. Omura, and H. Kikuchi. "Lactacystin, a Specific Inhibitor of the Proteasome, Induces Apoptosis in Human Monoblast U937 Cells." *Biochem Biophys Res Commun* 217.3 (1995): 1070-7. Print.

Rizq, Ola, Naoya Mimura, Motohiko Oshima, Atsunori Saraya, Shuhei Koide, Yuko Kato, Kazumasa Aoyama, Yaeko Nakajima-Takagi, Changshan Wang, and Anqi Ma. "Molecular Mechanism Behind the Synergistic Activity of Proteasome Inhibition and Prc2 Inhibition in the Treatment of Multiple Myeloma." American Society of Hematology Washington, DC, 2016. Print.

Rizq, Ola, Naoya Mimura, Shuhei Koide, Anqi Ma, Jian Jin, Tohru Iseki, Chiaki Nakaseko, and Atsushi Iwama. "Ezh2 Inhibition and the Combination with Proteasome Inhibition Are Novel Potential Strategies for the Treatment of Multiple Myeloma." American Society of Hematology Washington, DC, 2014. Print.

Lee, Susan J, Konstantin Levitsky, Francesco Parlati, Mark K Bennett, Shirin Arastu-Kapur, Lois Kellerman, Tina F Woo, Alvin F Wong, Kyriakos P Papadopoulos, and Ruben Niesvizky. "Clinical Activity of Carfilzomib Correlates with Inhibition of Multiple Proteasome Subunits: Application of a Novel Pharmacodynamic Assay." *British journal of haematology* 173.6 (2016): 884-95. Print.